MATERIALS AND METHODS

Subjects

Cerebrospinal fluid samples from 24 AD patients (mild to moderate AD; 50–86 years old), 19 MCI patients (57–82 years old) and 21 control subjects (61–89 years old) were collected (see Table 1) at Department of Neurology, Hirosaki University Hospital and at Department of Geriatrics and Gerontology, Tohoku University Hospital, and at Department of Neurology, Niigata University Hospital. The CSF samples from (symptomatic) 5 FAD (mPS1) patients (T116N, L173F, G209R, L286V and L381V) were from Niigata University Hospital. Probable AD cases met the criteria of the National Institute of Neurological and Communicative Disorders and Stroke–Alzheimer's Disease and Related Disorders (NINCDS-ADRDA) (Kuwano et al, 2006; McKhann et al, 1984). Additional diagnostic procedures included magnetic resonance imaging. Dementia severity was evaluated by the Mini-Mental State Examination (MMSE). Diagnosis of MCI was made according to the published criteria (Winblad et al, 2004). Diagnosis of iNPH was made according to the guideline issued by the Japanese Society of NPH (Ishikawa et al, 2008). Controls who had no sign of dementia and lived in an unassisted manner in the local community were recruited. All individuals included in this study were Japanese and 24 AD patients examined here were judged to have sporadic AD because of negative family history. This study was approved by the ethics committee at each hospital or institute.

Human cortical specimens for quantification of raft-associated γ-secretase activity were obtained from those brains that were removed, processed and placed in −80°C within 12 h postmortem [Patients were placed in a cold (4°C) room within 2 h after death] at the Brain Bank at Tokyo Metropolitan Institute of Gerontology. For all the brains registered at the bank we obtained written informed consents for their use for medical research from patient or patient's family. Each brain specimen (~0.5 g) were taken from Brodmann areas 9–11 of 13 AD patients [80 ± 5.0 years of age, Braak NFT stage > IV, SP stage = C (retrospective) CDR ≫ 1], 10 MCI patients (91 ± 4.9 years of age, Braak NFT stage < IV, SP stage < C, CDR = 0.5) and 16 controls (77 ± 6.5 years of age, Braak NFT stage < I, SP stage = 0/A, CDR = 0) (Adachi et al, 2010; Li et al, 1997).

Cerebrospinal fluid analysis

Cerebrospinal fluid (10–15 ml) was collected in a polypropylene or polystyrene tube and gently inverted. After brief centrifugation CSF was aliquotized to polypropylene tubes (0.25–0.5 ml), which were kept at −80°C until use. In our experience, Aβ42 (possibly, other Aβ species too) are readily absorbed even to polypropylene tubes (~20% per new exposure, as shown by Luminex xMAP quantification), and repeated aliquotization to new tubes may cause profoundly lower measures of Aβs (Tsukie and Kuwano, unpublished data, 2010). This may partly explain why absolute levels of Aβs in CSF greatly vary among laboratories, whereas their relative ratios (*e.g.* Aβ42/40) seem to be roughly consistent. The CSF concentrations of Aβ38, 40 and 42 were quantified using commercially available ELISA kits (Cat no. 27717, 27718 and 27712, respectively, IBL, Gunma, Japan). To measure Aβ43, anti-Aβ43 polyclonal antibody as a capture antibody was combined with amino terminus-specific antibody (82E1) (Cat no. 10323, IBL, Gunma, Japan) as a detector antibody. The detection limit of Aβ43 quantified by the ELISA was 0.78 pM (data not shown). Thus all ELISAs used here detect Aβ1-x, but not amino-terminally truncated Aβs. The specificities of ELISAs are provided in Supporting Information Fig S1.

CSF immunoprecipitation and Western blotting

When required, CSF Aβs were immunoprecipitated with protein G-sepharose conjugated with 82E1 at 4°C by keeping a container in gentle rotation overnight. The mixture was centrifuged at 10,000×g for 5 min, and resultant pellets were then washed twice with phosphate-buffered saline. The washed beads were suspended with the Laemmli sample buffer for SDS–polyacrylamide gel electrophoresis (SDS–PAGE). The immunoprecipitated Aβs were separated on Tris/Tricine/8 M urea gels (Kakuda et al, 2006), followed by Western blotting using 82E1. To immunodetect Aβ42 and Aβ43, Aβ42 monoclonal antibody (44A3, IBL) and Aβ43 polyclonal antibody (IBL) were used (Supporting Information Fig S3).

Numerical simulation based on the stepwise processing model of γ-secretase

The temporal profiles for the ratios of Aβ40/43 and Aβ38/42 were simulated based on the stepwise processing model. Parameters including rate constants were set to fit maximally the temporal profile of the cleaving activity in the reconstituted γ-secretase system (Takami et al, 2009).

We set the condition that βCTF substrate is supplied steadily from the external source. When βCTF supply is balanced roughly in the order with γ-secretase processing rate, the stepwise-processing model was found to have the two successive steady states, with each accompanying linear changes in [ES] or [S] concentrations. The first steady state is just after the initial transition period that corresponds to the acute saturation phase of γ-secretase with βCTF. The second steady state is associated with the constant concentrations of the enzyme/substrate complex except ES38 and ES40. Because these steady states kept the ratios of Aβ38/Aβ40 and Aβ42/Aβ43 constant, the simulation was quite consistent with the CSF data.

Quantification of human brain raft-associated γ-secretase activity

Since γ-secretase is thought to be concentrated in rafts (Hur et al, 2008; Wada et al, 2003), we measured raft-associated γ-secretase activity rather than CHAPSO-solubilized activity. Rafts were prepared from human brains which were frozen within 12 h postmortem, as previously described (Oshima et al, 2001; Wada et al, 2003) with some modifications. We do not know exactly whether the γ-secretase activity depends upon the sampling site. In our hands, there appear no large differences in the activity among the sampled sites in a given prefrontal slice. No significant differences in the activity were noted between outer and inner layer of the cortex. After carefully removing leptomeninges and blood vessels, small (<0.5 g) blocks from prefrontal cortices (Brodmann areas 9–11) were homogenized in ~10 volumes of 10% sucrose in MES-buffered saline (25 mM MES, pH 6.5, and 150 mM NaCl) containing 1% CHAPSO and various protease inhibitors. The homogenate was adjusted to 40% sucrose by the addition of an equal volume of 70% sucrose in MES-buffered saline, placed at the bottom of an ultracentrifuge tube, and overlaid with 4 ml of 35% sucrose and finally with 4 ml of 5% sucrose in MES-buffered saline. The discontinuous gradient was centrifuged at 39,000 rpm for 20 h at 4°C on a SW 41 Ti rotor (Beckman, Palo

The paper explained

PROBLEM:

Alzheimer's disease is a devastating form of progressive dementia, in which senile plaques composed of Aβ form in the brain. Different species of Aβ are derived from APP through sequential cleavage by β- and γ-secretases and can be detected in the CSF of patients. These can serve as markers for the disease.

RESULTS:

We investigated why CSF concentrations of Aβ42 are lower in MCI and AD patients. We suggest that this is not because Aβ42/43 is selectively deposited in the brain, but because γ-secretase activity is altered in AD brain: more Aβ42 and Aβ43 are converted to Aβ40 and Aβ38, respectively, resulting in lower Aβ42 and Aβ43 in CSF.

IMPACT:

Our results predict that γ-secretase modulators would have only limited efficacy in treatment of AD patients, because Aβ42/43 production by γ-secretase is already shifted towards reduced levels in AD brain.

Alto, CA). An interface of 5%/35% sucrose (fraction 2) was carefully collected (referred to as raft fraction). Raft fractions were recentrifuged after dilution with buffer C (20 mM PIPES, pH 7.0, 250 mM sucrose and 1 mM EGTA). The resultant pellet was washed twice and resuspended with buffer C, which was kept at −80°C until use.

As the method of measuring the raft γ-secretase activity was not yet established, we first determined the assay conditions. The incubation of raft fraction with βCTF generated exactly the same tri- and tetrapeptides we previously observed in the detergent-soluble γ-secretase assay system (Takami et al, unpublished observation). This suggests that the cleavage by raft-associated γ-secretase proceeds in the identical manner as by CHAPSO-reconstituted γ-secretase (Takami et al, 2009). In our hands, preexisting βCTF bound in rafts generated only negligible amounts of Aβs, and their generation was dependent exclusively on exogenously added βCTF. Thus, we concluded that the addition of βCTF to raft fraction make possible to measure the raft-associated γ-secretase activity, although we do not know how the exogenously added βCTF is integrated into raft, gets access to and is degraded by raft-embedded γ-secretase. Using this assay method, the activities of raft-associated γ-secretase in human brains were found to be only a little affected postmortem, when compared with that prepared from fresh rat brains. A progressive decline in the activity was barely detectable from 4 to 17 h postmortem. The discrepancy in the postmortem decay between our and the previous data (Hur et al, 2008) would be ascribed to the assay method: the latter are based on the activity measured by using endogenous (raft-bound) substrate that is also susceptible to proteolytic degradation (Hur et al, 2008).

Each raft fraction, adjusted to 100 μg/ml in protein concentration, was incubated with 200 nM C99FLAG for 2 h at 37°C (Kakuda et al, 2006). The produced Aβs were separated on SDS–PAGE, and subjected to quantitative Western blotting, using specific antibodies, 3B1 for Aβ38, BA27 for Aβ40, 44A3 for Aβ42 and anti-Aβ43 polyclonal for Aβ43.

Statistical analysis

All statistical analyses were performed using SPSS version 14.0. The results were expressed as means ± standard deviations. Because data transformations were required to achieve normally distributed data, all analyses including Aβ38, Aβ40, Aβ42 and Aβ43 were performed after a logarithmic transformation. Pearson's correlation coefficients were calculated to indicate the strength of the linear relationship between two variables. An ANOVA was used to test the equality of mean values of continuous variables among three groups, that is control, MCI and AD. Multiple comparisons were done by Dunnett's *t*-test, Bonferroni's *t*-test and Welch's *t*-test between control and MCI/AD, and among three groups, respectively. A two-tailed *p*-value of <0.05 was considered to be statistically significant.

Author contributions

NK, MT, KN, YI: measurement of raft-associated γ-secretase activity in human brains, LC-MS/MS confirmation of released peptides, ELISA quantification of Aβ38, 40, 42 and 43 in CSF and tissue blocks, and experimental design of the present work; MS, HiA, KF, TI, and the Japanese Alzheimer's Disease Neuroimaging Initiative: collection of CSF samples from controls, MCI/AD patients; YH, MM, HaA: collection of CSF from iNPH patients; HY, SM, HH: Aβ immunocytochemistry of tissue sections from brains with various SP stages (Braak); KA: statistical analysis; RK: establishment of the appropriate Aβ quantification conditions; YN: simulation of the stepwise processing model.

Acknowledgements

We thank Dr. Haruhiko Akiyama, Department of Psychogeriatrics, Tokyo Institute of Psychiatry, Tokyo Metropolitan Organization for Medical Research, Tokyo, for the help in the initial phase of this study, and Dr. Takaomi C. Saido, RIKEN Brain Science Institute, for sharing the data on his R278I transgenic mice. Dr. Makoto Higuchi, Molecular Imaging Center, National Institute of Radiological Sciences, Chiba, kindly provided us with aged Tg2576 littermates. This project was supported by New Energy and Industrial Technology Development Organization in Japan (J-ADNI).

Supporting Information is available at EMBO Molecular Medicine online.

The authors declare that they have no conflict of interest.

References

Adachi T, Saito Y, Hatsuta H, Funabe S, Tokumaru AM, Ishii K, Arai T, Sawabe M, Kanemaru K, Miyashita A, *et al* (2010) Neuropathological asymmetry in argyrophilic grain disease. J Neuropathol Exp Neurol 69: 737-744

Hong S, Quintero-Monzon O, Ostaszewski BL, Podlisny DR, Cavanaugh WT, Yang T, Holtzman DM, Cirrito JR, Selkoe DJ (2011) Dynamic analysis of amyloid β-protein in behaving mice reveals opposing changes in ISF versus parenchymal Aβ during age-related plaque formation. J Neurosci 31: 15861-15869

Hur JY, Welander H, Behbahani H, Aoki M, Frånberg J, Winblad B, Frykman S, Tjernberg LO (2008) Active gamma-secretase is localized to detergent-resistant membranes in human brain. FEBS J 275: 1174-1187

Ishikawa M, Hashimoto M, Kuwana N, Mori E, Miyake H, Wachi A, Takeuchi T, Kazui H, Koyama H (2008) Guidelines for management of idiopathic normal pressure hydrocephalus. Neurol Med Chir (Tokyo) 48: S1-S23

Iwatsubo T, Odaka A, Suzuki N, Mizusawa H, Nukina N, Ihara Y (1994) Visualization of Aβ42(43) and Aβ40 in senile plaque with end-specific Aβ monoclonals: evidence that an initially deposited forms is Aβ42(43). Neuron 13: 45-53

Kakuda N, Funamoto S, Yagishita S, Takami M, Osawa S, Dohmae N, Ihara Y (2006) Equimolar production of amyloid β-protein and amyloid precursor protein intracellular domain from β-carboxyl-terminal fragment by γ-secretase. J Biol Chem 281: 14776-14786

Kawarabayashi T, Younkin LH, Saido TC, Shoji M, Ashe KH, Younkin SG (2001) Age-dependent changes in brain, CSF, and plasma amyloid (β) protein in the Tg2576 transgenic mouse model of Alzheimer's disease. J Neurosci 21: 372-381

Kosaka T, Imagawa M, Seki K, Arai H, Sasaki H, Tsuji S, Asami-Odaka A, Fukushima T, Imai K, Iwatsubo T (1997) The βAPP717 Alzheimer mutation increases the percentage of plasma amyloid-beta protein ending at Aβ42(43). Neurology 48: 741-745

Kuwano R, Miyashita A, Arai H, Asada T, Imagawa M, Shoji M, Higuchi S, Urakami K, Kakita A, Takahashi H, *et al* (2006) Dynamin-binding protein gene on chromosome 10q is associated with late-onset Alzheimer's disease. Hum Mol Genet 15: 2170-2182

Li G, Aryan M, Silverman JM, Haroutunian V, Perl DP, Birstein S, Lantz M, Marin DB, Mohs RC, Davis KL (1997) The validity of the family history method for identifying Alzheimer disease. Arch Neurol 54: 634-640

McKhann G, Drachman D, Folstein M, Katzman R, Price D, Stadlan EM (1984) Clinical diagnosis of Alzheimer's disease: report of the NINCDS-ADRDA Work Group under the auspices of Department of Health and Human Services Task Force on Alzheimer's Disease. Neurology 34: 939-944

Nakaya Y, Yamane T, Shiraishi H, Wang HQ, Matsubara E, Sato T, Dolios G, Wang R, De Strooper B, Shoji M, *et al* (2005) Random mutagenesis of presenilin-1 identifies novel mutants exclusively generating long amyloid β-peptides. J Biol Chem 280: 19070-19077

Oshima N, Morishima-Kawashima M, Yamaguchi H, Yoshimura M, Sugihara S, Khan K, Games D, Schenk D, Ihara Y (2001) Accumulation of amyloid beta-protein in the low-density membrane domain accurately reflects the extent of beta-amyloid deposition in the brain. Am J Pathol 158: 2209-2218

Qi-Takahara Y, Morishima-Kawashima M, Tanimura Y, Dolios G, Hirotani N, Horikoshi Y, Kametani F, Maeda M, Saiso TC, Wang R, *et al* (2005) Longer forms of amyloid β protein: implications for the mechanism of intramembrane cleavage by γ-secretase. J Neurosci 25: 436-445

Ringman JM, Younkin SG, Pratico D, Seltzer W, Cole GM, Geschwind DH, Rodriguez-Agudelo Y, Schaffer B, Fein J, Sokolow S, *et al* (2008) Biochemical markers in persons with preclinical familial Alzheimer disease. Neurology 71: 85-92

Saito T, Suemoto T, Brouwers N, Sleegers K, Funamoto S, Mihira N, Matsuba Y, Yamada K, Nilsson P, Takano J, *et al* (2011) Potent amyloidogenicity and pathogenicity of Aβ43. Nat Neurosci 14: 1023-1032

Scheuner D, Eckman C, Jensen M, Song X, Citron M, Suzuki N, Bird TD, Hardy J, Hutton M, Kukull W, *et al* (1996) Secreted amyloid β-protein similar to that in the senile plaques of Alzheimer's disease in increase in vivo by the presenilin 1 and 2 and APP mutations linked to familial Alzheimer's disease. Nat Med 2: 864-870

Schoonenboom NS, Mulder C, Van Kamp GJ, Mehta SP, Scheltens P, Blankenstein MA, Mehta PD (2005) Amyloid β 38, 40, and 42 species in cerebrospinal fluid: more of the same. Ann Neurol 58: 139-142

Selkoe DJ (2001) Alzheimer's disease: genes, proteins, and therapy. Physiol Rev 81: 741-766

Serneels L, Van Biervliet J, Craessaerts K, Dejaegere T, Horre K, Van Houtvin T, Esselmann H, Paul S, Schafer MK, Berezovska O, *et al* (2009) γ-Secretase heterogeneity in the Aph1 subunit: relevance for Alzheimer's disease. Science 324: 639-642

Shoji M, Matsubara E, Kanai M, Watanabe M, Nakamura T, Tomidokoro Y, Shizuka M, Wakabayashi K, Igeta Y, Ikeda Y, *et al* (1998) Combination assay of CSF tau, Aβ1–40 and Aβ 1–42(43) as a biochemical marker of Alzheimer's disease. J Neurol Sci 158: 134-140

Silverberg GD, Mayo M, Saul T, Rubenstein E, McGuire D (2003) Alzheimer's disease, normal-pressure hydrocephalus, and senescent changes in CSF circulatory physiology: a hypothesis. Lancet Neurol 2: 506-511

Simonsen AH, Hansson SF, Ruetschi U, McGuire J, Podust VN, Davies HA, Mehta P, Waldemar G, Zetterberg H, Andreasen N, *et al* (2007) Amyloid β1–40 quantification in CSF: comparison between chromatographic and immunochemical methods. Dement Geriatr Cogn Disord 23: 246-250

Takami M, Nagashima Y, Sano Y, Ishihara S, Morishima-Kawashima M, Funamoto S, Ihara Y (2009) γ-Secretase: successive tripeptide and tetrapeptide release from the transmembrane domain of β-carboxyl terminal fragment. J Neurosci 29: 13042-13052

Takasugi N, Tomita T, Hayashi I, Tsuruoka M, Niimura M, Takahashi Y, Thinakaran G, Iwatsubo T (2003) The role of presenilin cofactors in the γ-secretase complex. Nature 422: 438-441

Wada S, Morishima-Kawashima M, Qi Y, Misonou H, Shimada Y, Ohno-Iwashita Y, Ihara Y (2003) Gamma-secretase activity is present in rafts but is not cholesterol-dependent. Biochemistry 47: 13977-13986

Weggen S, Eriksen JL, Das P, Sagi SA, Wang R, Pietrzik CU, Findlay KA, Smith TE, Murphy MP, Bulter T, *et al* (2001) A subset of NSAIDs lower amyloidogenic Aβ42 independently of cyclooxygenase activity. Nature 414: 212-216

Winblad B, Palmer K, Kivipelto M, Jelic V, Fratiglioni L, Wahlund LO, Nordberg A, Backman L, Albert M, Almkvist O, *et al* (2004) Mild cognitive impairment—beyond controversies, towards a consensus: report of the International Working Group on Mild Cognitive Impairment. J Intern Med 256: 240-246

Yang DS, Tandon A, Chen F, Yu G, Yu H, Arakawa S, Hasegawa H, Duthie M, Schmidt SD, Ramabhadran TV, *et al* (2002) Mature glycosylation and trafficking of nicastrin modulate its binding to presenilins. J Biol Chem 277: 28135-28142

Zou K, Yamaguchi H, Akatsu H, Sakamoto T, Ko M, Mizoguchi K, Gong JS, Yu W, Yamamoto T, Kosaka K, *et al* (2007) Angiotensin-converting enzyme converts amyloid β-protein 1–42 (Aβ(1–42)) to Aβ(1–40), and its inhibition enhances brain Aβ deposition. J Neurosci 27: 8628-8635

NEUROPATHOLOGY

Neuropathology 2012; **32**, 595–603 doi:10.1111/j.1440-1789.2012.01302.x

Original Article

Reduced brain-derived neurotrophic factor (BDNF) mRNA expression and presence of BDNF-immunoreactive granules in the spinocerebellar ataxia type 6 (SCA6) cerebellum

Makoto Takahashi,[1] Kinya Ishikawa,[1] Nozomu Sato,[1] Masato Obayashi,[1] Yusuke Niimi,[1] Taro Ishiguro,[1] Mitsunori Yamada,[4,5] Yasuko Toyoshima,[4] Hitoshi Takahashi,[4] Takeo Kato,[6] Masaki Takao,[7,*] Shigeo Murayama,[3] Osamu Mori,[8] Yoshinobu Eishi[2] and Hidehiro Mizusawa[1]

Departments of [1]Neurology and Neurological Science and [2]Pathology, Graduate School, Tokyo Medical and Dental University, [3]Department of Neuropathology (The Brain Bank for Aging Research), Tokyo Metropolitan Geriatric Hospital and Institute of Gerontology, Tokyo, [4]Department of Pathology, Pathological Neuroscience Branch, Brain Research Institute, Niigata University, [5]Department of Clinical Research, National Hospital Organization, Saigata National Hospital, Niigata, [6]Department of Neurology, Hematology, Metabolism, Endocrinology and Diabetology (DNHMED), Yamagata University Faculty of Medicine, Yamagata, [7]Department of Neurology, Institute of Brain and Blood Vessels, Mihara Memorial Hospital, Gunma, and [8]Department of Internal Medicine and Neurology, Hatsuishi Hospital, Chiba, Japan

Spinocerebellar ataxia type 6 (SCA6) is an autosomal-dominant neurodegenerative disorder caused by a small expansion of tri-nucleotide (CAG) repeat encoding polyglutamine (polyQ) in the gene for α_{1A} voltage-dependent calcium channel ($Ca_v2.1$). Thus, this disease is one of the nine neurodegenerative disorders called polyQ diseases. The Purkinje cell predominant neuronal loss is the characteristic neuropathology of SCA6, and a 75-kDa carboxy-terminal fragment (CTF) of $Ca_v2.1$ containing polyQ, which remains soluble in normal brains, becomes insoluble in the cytoplasm of SCA6 Purkinje cells. Because the suppression of the brain-derived neurotrophic factor (BDNF) expression is a potentially momentous phenomenon in many other polyQ diseases, we implemented BDNF expression analysis in SCA6 human cerebellum using quantitative RT-PCR for the *BDNF* mRNA, and by immunohistochemistry for the BDNF protein. We observed significantly reduced *BDNF* mRNA levels in SCA6 cerebellum ($n = 3$) compared to controls ($n = 6$) (Mann–Whitney *U*-test, $P = 0.0201$). On immunohistochemistry, BDNF protein was only weakly stained in control cerebellum. On the other hand, we found numerous BDNF-immunoreactive granules in dendrites of SCA6 Purkinje cells. We did not observe similar BDNF-immunoreactive granules in other polyQ diseases, such as Huntington's disease or SCA2. As we often observed that the 1C2-positive $Ca_v2.1$ aggregates existed more proximally than the BDNF-positive granules in the dendrites, we speculated that the BDNF protein trafficking in dendrites may be disturbed by $Ca_v2.1$ aggregates in SCA6 Purkinje cells. We conclude that the SCA6 pathogenic mechanism associates with the *BDNF* mRNA expression reduction and abnormal localization of BDNF protein.

Key words: brain–derived neurotrophic factor (BDNF), immunohistochemistry, Purkinje cell, quantitative reverse transcription PCR (qRT-PCR), spinocerebellar ataxia type 6 (SCA6).

Correspondence: Kinya Ishikawa, MD, PhD, Department of Neurology and Neurological Science, Graduate School, Tokyo Medical and Dental University, 1-5-45, Yushima, Bunkyo-ku, Tokyo 113-8510, Japan. Email: pico.nuro@tmd.ac.jp

*Present address: Department of Neuropathology (The Brain Bank for Aging Research), Tokyo Metropolitan Geriatric Hospital and Institute of Gerontology, 35-2, Sakaecho, Itabashi-ku, Tokyo 173-0015, Japan.

Received 22 December 2011; revised 19 January 2012 and accepted 20 January 2012; published online 7 March 2012.

INTRODUCTION

Spinocerebellar ataxia type 6 (SCA6) is an autosomal-dominant neurodegenerative disorder clinically characterized by progressive cerebellar ataxia and gaze-evoked nystagmus with an average age of onset at 45.5 years.[1,2] The disease is caused by an expansion of the tri-nucleotide (CAG) repeat encoding polyglutamine (polyQ) in the gene for the α_{1A} (P/Q-type) voltage-dependent calcium channel protein ($Ca_v2.1$).[3] Thus, SCA6 is one of the polyQ diseases which consist of nine inherited neurological disorders caused by an expansion of the polyQ tract in the causative protein. The polyQ expansion causing SCA6 exists in the cytoplasmic carboxyl(C)-tail of the $Ca_v2.1$.[3] The Purkinje cell of the cerebellar cortex, which expresses $Ca_v2.1$ most abundantly in the brain, undergoes predominant degeneration.[2,4] Although it is not clear how the polyQ expansion in $Ca_v2.1$ causes the disease, $Ca_v2.1$ aggregation specifically observed in the SCA6 Purkinje cells is likely to harbor a clue.[4,5]

SCA6 has some unique features distinct from other polyQ diseases. First, the length of the polyQ tract expansion responsible for SCA6 is remarkably short and falls within the normal range of repeats for other polyQ diseases. The lengths of CAG repeats/polyQ tract are 20–33 repeats in SCA6 patients,[6,7] while they are required to be larger than 35 repeats for being causative in other polyQ diseases such as Huntington's disease (HD).[8] Second, microscopic $Ca_v2.1$ aggregates can be seen mainly in the cytoplasm (the cell body and cell processes) of SCA6 Purkinje cells, whereas in other polyQ diseases, aggregates with expanded polyQ are prevalent in the nuclei rather than in the cytoplasm of neurons expressing the responsible proteins.[9,10] These could indicate that the pathophysiology underlying SCA6 is quite different form that of other polyQ diseases.

The brain-derived neurotrophic factor (BDNF) is a multifunctional trophic factor expressed broadly in the CNS.[11] On the other hand, the brains affected with other polyQ diseases show a reduction in the BDNF gene expression. For example, the caudate nucleus and putamen of HD brains show reduced BDNF gene expression.[12] One of the possible mechanisms underlying this reduction is the sequestration of the cyclic-AMP responsive element binding protein (CREB)-binding protein (CBP) by the expanded polyQ in the neuronal nuclei, leading to the suppression of the CREB transcription, resulting in the reduction of BDNF transcription.[13] There may be another mechanism in HD. The wild-type huntingtin activates BDNF transcription in cultured CNS neurons by a pathway independent of CREB. However, the mutated huntingtin with expanded polyQ does not activate this pathway,[14] resulting in reduced BDNF transcription. Interestingly, overexpression of the BDNF in the striatum mitigates symptoms of HD in mice,[15] suggesting that the reduction of BDNF may be a substrate for therapy of polyQ diseases.

From these backgrounds, we carried out quantitative reverse transcription PCR (qRT-PCR) analysis to assess *BDNF* mRNA expression levels, and immunohistochemistry for investigating BDNF protein localization, both to see whether expression of BDNF is also altered in SCA6 cerebellum. Given that the reduced *BDNF* mRNA expression is determined by the sequestration of CBP in affected neuronal nuclei,[16–18] SCA6 brains may not show BDNF reduction, since nuclear $Ca_v2.1$ aggregates are very few in SCA6. However, we found that *BDNF* mRNA is also suppressed in SCA6 cerebellum. Interestingly, we also found that the BDNF protein forms definable granules in the SCA6 Purkinje cell dendrites. Here, we show that BDNF expression is abnormal in SCA6 human cerebellum.

MATERIALS AND METHODS

Specimens

Brain specimens obtained at autopsy with family consent were investigated. For assessing mRNA levels by qRT-PCR, three SCA6 and six control cerebellar tissues were examined (Table 1). These six controls were from individuals without obvious neurological diseases obtained from the Research Network of Aging Brain Research, Tokyo Metropolitan Geriatric Hospital and Institute of Gerontology. For immunohistochemistry, we studied five SCA6 patients, nine controls including three HD, one for each SCA2, SCA3/Machado-Joseph disease (MJD), dentatorubral and pallidoluysian atrophy (DRPLA), one Parkinson's disease, and two SCA31 patients (Table 1). The brains were fixed in formalin, and tissue sections were embedded in paraffin. Six-micron-thick sections were used for staining.

The study was approved by the institutional review boards of ethics of Tokyo Medical and Dental University and Tokyo Metropolitan Geriatric Hospital and Institute of Gerontology, and conformed to the tenets of the Declaration of Helsinki.

RNA extraction and qRT-PCR

Human brain tissues of the cerebellar hemispheric cortices, kept frozen at −80°C after autopsy, were dissected. Total RNA was isolated from each individual by TRIzol (Invitrogen, Carlsbad, CA, USA) and RNeasy mini kit (Qiagen, Valencia, CA, USA) according to the manufacturer's protocol. Then the total RNA was treated with DNase (Invitrogen) and quantified on a nanodrop spectrophotometer (Thermo Scientific, Wilmington, DE, USA). Reverse tran-

Table 1 Profiles of the investigated patients

Diagnosis	Individual no.	Age at death (years)/gender	Repeat size	Investigations
SCA6				
SCA6	Pt. 1	75/female	13/22	qRT-PCR, IHC
SCA6	Pt. 2	76/female	13/22	qRT-PCR, IHC
SCA6	Pt. 3	66/male	15/22	qRT-PCR, IHC
SCA6	Pt. 4	79/female	13/22	IHC
SCA6	Pt. 5	68/female	13/22	IHC
Controls				
Non-neurological	Ct. 1	57/male	Not examined	qRT-PCR
Non-neurological	Ct. 2	57/male	Not examined	qRT-PCR
Non-neurological	Ct. 3	62/male	Not examined	qRT-PCR
Non-neurological	Ct. 4	62/male	Not examined	qRT-PCR
Non-neurological	Ct. 5	90/male	Not examined	qRT-PCR
Non-neurological	Ct. 6	92/male	Not examined	qRT-PCR
Huntington's disease	Ct. 7	48/female	Not examined	IHC
Huntington's disease	Ct. 8	52/male	Not examined	IHC
Huntington's disease	Ct. 9	72/female	Not examined	IHC
SCA2	Ct.10	67/male	Not examined	IHC
Machado-Joseph disease	Ct.11	65/male	Not examined	IHC
Dentatorubral & pallidoluysian atrophy	Ct.12	58/female	Not examined	IHC
Parkinson's disease	Ct.13	88/male	Not examined	IHC
SCA31	Ct.14	74/male	11/13.	IHC
SCA31	Ct.15	79/male	11/14.	IHC

IHC, immunohistochemistry; qRT-PCR, quantitative reverse-transcription polymerase chain reaction.

scription generating complementary DNA (cDNA) was carried out with random hexmers and deoxy-thymidine oligomers (oligo-dT) mixtures using a PrimeScript™ RT Master Mix (TaKaRa Bio, Tokyo, Japan). The *BDNF* and glyceraldehyde-3-phophate degydrogenase (*GAPDH*) mRNA TaqMan® Gene Expression Assays ([BDNF] = Hs00380947 = m1, [GAPDH] = 4333764T) (Applied Biosystems, Foster City, CA, USA) were purchased, and qRT-PCR was performed by LightCycler 480II (Roche, Basel, Switzerland). The *BDNF* mRNA levels were calculated against the *GAPDH* mRNA expression levels in each sample.

The *BDNF* mRNA/*GAPDH* mRNA expression ratios were calculated using the delta-delta threshold cycle (Ct) method, and were compared between controls and SCA6 group. A standard *BDNF* mRNA/*GAPDH* mRNA ratio in one control subject was expressed as 1 (standard caliber) while the rest of the samples were presented with relative values to this standard. Each experiment was repeated three times independently and was averaged (mean ± SD). Finally, the controls ($n = 6$) and SCA6 ($n = 3$) groups were compared using Mann–Whitney *U*-test.

Immunohistochemistry of human brain tissues

Immunohistochemistry was carried out as described previously.[4,5,19] For antigen retrieval, tissue blocks were boiled by exposing microwaves three times for 1 min in 10 mmol citrate buffer (pH 7.4), rinsed in distilled water and then immersed in folic acid for 5 min. Sections were incubated overnight at 4°C with one of the following three antibodies: anti-BDNF antibody (rabbit polyclonal, sc546 [alternatively named N-20],[12] diluted at 1:100 with PBS ph7.4) (Santa Cruz Biotechnology, Santa Cruz, CA, USA), 1C2 for the expanded polyQ tracts (mouse monoclonal, 5TF1-1C2, 1:4000) (Millipore, Temecula, CA, USA), and A6RPT-#5803 for $Ca_v2.1$ C-terminal region (rabbit polyclonal, 1:500).[19] The primary antibodies were serially detected with the Vectastain ABC rabbit or mouse IgG kits (Vector Laboratories, Burlingame, CA, USA), and visualized by using Histofine Simple Stain DAB (Nichirei Bioscience, Tokyo, Japan) according to the manufacturer's protocol.

For double immunofluorescent labeling, sections were similarly treated as above and incubated with primary antibodies overnight at 4°C with anti-BDNF antibody (rabbit polyclonal, 1:50) (Santa Cruz Biotechnology) and 1C2 antibody (mouse monoclonal, 5TF1-1C2, 1:2000; Millipore). Sections were washed three times in PBS and incubated with fluoresecein-labeled anti-mouse IgG (heavy and light chains [H + L]) (1:250) (Vector Laboratories) and Alexa-fluor 555 goat anti-rabbit IgG (H + L) (1:250) (Invitorogen) for 1 h at room temperature. Sections were washed three times in PBS, incubated with 1% Sudan black B in 70% methanol for 5 min to reduce the autofluorescence, washed three times in PBS and incubated with 3% 4′,6-diamidino-2-phenylindole solution for 15 min at 37°C. Slides were observed under a confocal microscope (LSM 510META; Carl Zeiss, Jena, Germany).

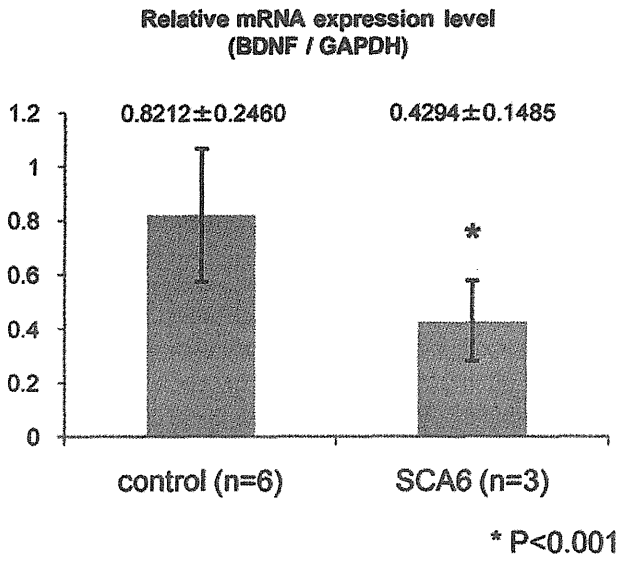

Fig. 1 Brain-derived neurotrophic factor (BDNF) expression level in spinocerebellar ataxia type 6 (SCA6) patients' cerebella is decreased in comparison with that in control patients' cerebella. Quantitative (q) RT-PCR reveals that the level of BDNF mRNA against that of glyceraldehyde 3-phosphate dehydrogenase (GAPDH) is significantly reduced in SCA6 cerebellum ($n = 3$) in comparison with controls ($n = 6$). (Control, ($n = 6$: 0.8212 ± 0.2460; SCA6, $n = 3$: 0.4294 ± 0.1485; $P = 0.0201$).

RESULTS

The *BDNF* mRNA expression level is decreased in SCA6 human cerebellum

The qRT-PCR analysis on each cDNA generated from SCA6 ($n = 3$) and control ($n = 6$) cerebellar tissues revealed that the level of *BDNF* mRNA against that of *GAPDH* mRNA was significantly reduced in SCA6 human cerebellum compared to controls (controls $n = 6$: 0.8212 ± 0.2460; SCA6, $n = 3$: 0.4294 ± 0.1485; $P = 0.0201$) (Fig. 1). This suggests that the *BDNF* mRNA expression level is decreased in SCA6 cerebellar cortex.

Observation of BDNF-immunoreactive granules in the dendrites of SCA6 Purkinje cells

To investigate whether there is a change for quantity and intracellular localization of BDNF protein in the SCA6 cerebellum, we undertook immunohistochemical analysis of SCA6 and control human cerebella with the anti-BDNF antibody. In control cerebellum, the BDNF-immunoreactivity was only weakly seen in all neurons, including the Purkinje cells and granule cells (Fig. 2a,b). The BDNF immunoreactivity was also quiescent in the SCA2 cerebellum (Fig. 2c), whereas 1C2-positive polyQ aggregates are seen in the Purkinje cell cytoplasm (Fig. 2d). In contrast, numerous BDNF-immunopositive granules were seen in the structures compatible with dendritic trees of SCA6 Purkinje cells (Fig. 2e,f, arrows). The BDNF granules were not conspicuous in the cell bodies (Fig. 2f, arrowhead) or axons of Purkinje cells. The antibody A6RPT-#5803 against the $Ca_v2.1$ C-terminus detected numerous $Ca_v2.1$ aggregates in the proximal dendrite (Fig. 2g, filled arrow) as well as in the cell body. Occasionally, they were present even in the distal part of the dendrites (Fig. 2g, open arrow), showing that the $Ca_v2.1$ aggregates exist in a wide range of dendritic arbors. The BDNF-positive structures similar to the ones seen in SCA6 Purkinje cells were sought in other areas of brains affected with polyQ diseases. However, we did not see any similar structures in as far as we investigated the cerebral cortex and the striatum of HD brains (Fig. 2h) and the pons of MJD patients. The present observation indicates that formation of BDNF-positive granules may be specific to SCA6 Purkinje cell dendrites.

BDNF-immunoreactive granules are observed in the vicinity of $Ca_v2.1$ aggregates

We next asked whether the presence of BDNF-immunoreactive granules is related to the formation of $Ca_v2.1$ aggregates known to be specific to SCA6 cell bodies and dendrites.[4,5,19] To address this question, we carried out a double immunofluorescence study against BDNF (red) and 1C2 (green).

We found that 1C2-positive polyQ aggregates often existed in the proximal portion of dendrites, such as the primary shaft (Fig. 3a, arrow) or the secondary shaft (Fig. 3b, arrow), of the Purkinje cells. On the other hand, the BDNF-immunoreactive structures were seen distal to the 1C2-positive polyQ aggregates (Fig. 3a,b). Curiously, we found that the BDNF-immunoreactive granules were seen not only within the contour of Purkinje cell dendrites (Fig. 3a,b), but also outside of the visible dendritic structures (Fig. 3c,d, arrowheads).

DISCUSSION

We made two fundamental observations in this study. One is the reduced *BDNF* mRNA level in the SCA6 cerebellum. The BDNF is a member of the neurotrophic family controlling many processes, including neurogenesis, proliferation, survival, synaptic transmission and activity-dependent synaptic plasticity.[11,13] The molecule is widely distributed in the CNS and is abundantly expressed in the cerebellar cortex, including Purkinje cells.[20] The BDNF appears to be involved in many polyQ diseases. In HD, reduced BDNF gene expression has been found in cultured cells,[14] an animal model,[15] and in patients' brains.[12,21] In addition, over-expression of BDNF gene in the striatum of

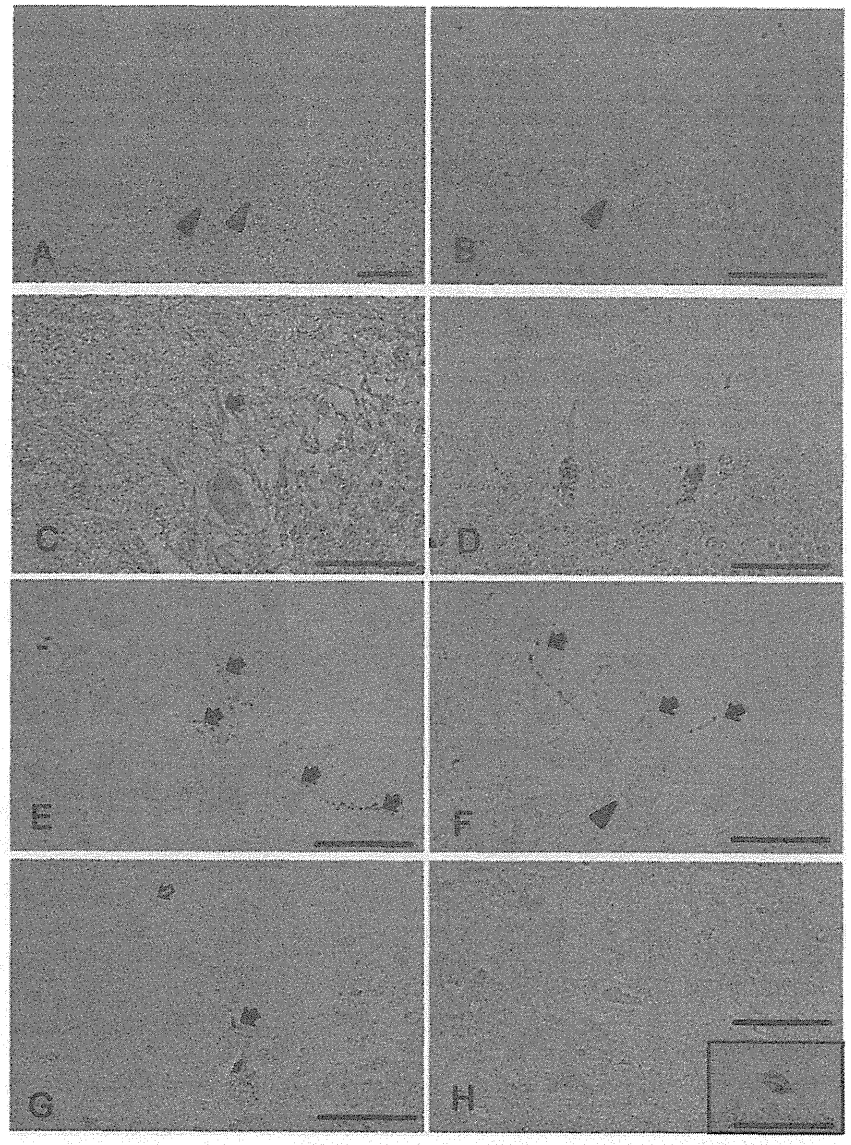

Fig. 2 Numerous brain-derived neurotrophic factor (BDNF)-immunoreactive granules are present in the dendrites of spinocerebellar ataxia type 6 (SCA6) Purkinje cells. (A, B) In control patients' cerebella, BDNF immunoreactivity is undetectable. Arrowheads indicate cell bodies of the Purkinje cells. (A, Parkinson's disease; B, SCA31). (C, D) In SCA2 cerebellum, BDNF immunoreactivity is also quiescent (C), but 1C2-positive granules are abundant in the Purkinje cell cytoplasm (D). (E, F) In a SCA6 Purkinje cell, numerous BDNF-immunoreactive granules are seen in the structures compatible with dendritic trees of Purkinje cells (arrows). BDNF granules are not conspicuous in the cell cytoplasm of Purkinje cells (arrowhead). (G) A6RPT-#5803 antibody, which is against α1A voltage-dependent calcium channel protein ($Ca_v2.1$) C-terminus, detects numerous $Ca_v2.1$ aggregates in the cell body of Purkinje cells and often in the proximal dendrite (filled arrow). $Ca_v2.1$ aggregates occasionally present even in the distal part of the dendrite (open arrow). (H) BDNF immunoreactivity is not seen in the striatum of Huntington's disease brains (large box), otherwise 1C2-positive aggregate are seen in the nuclei of striatal neurons (small box). (For A–G: scale bars; 50 μm).

HD mice compensates for reduced BDNF gene levels, ameliorating disease phenotypes.[15] The reduced BDNF gene expressions are also observed in a DRPLA cell model expressing mutant atrophin-1 and in SCA1 mouse models.[22,23] Interestingly, the drug 3,4-diaminopyridine improved motor behavior of mice by increasing BDNF expression levels.[23] These lines of evidence seem to indicate that BDNF has an important defence role in many polyQ diseases. The BDNF gene expression was also found to be reduced in affected areas of subjects with Alzheimer's disease[24] and Parkinson's disease,[25] suggesting that *BDNF* mRNA could be reduced in many neurodegenerative diseases. Considering that the BDNF is also abundantly expressed in Purkinje cells, it is possible to speculate that reduced BDNF gene expression in SCA6 cerebella may be related to the pathogenic mechanism of SCA6. However, the precise mechanism of BDNF mRNA reduction in SCA6 is not clear. While the presence of nuclear polyQ aggregates is causally associated with BDNF suppression in other polyQ diseases, such aggregates are extremely rare in SCA6 Purkinje cells.[5,19] Therefore, the mechanism reducing the BDNF gene expression in SCA6 may be different from other polyQ diseases. In cultured cell models, we recently found that the "cytoplasmic" $Ca_v2.1$ aggregates caused the reduction of CREB and phosphorylated(p)-CREB, the active CREB isoform, in the nuclei by sequestering them to the $Ca_v2.1$ aggregates in the cytoplasm (manuscript submitted). In SCA6 human brains, we also confirmed that CREB also co-localizes with $Ca_v2.1$ aggregates in Purkinje cell bodies. Thus, we speculate that the

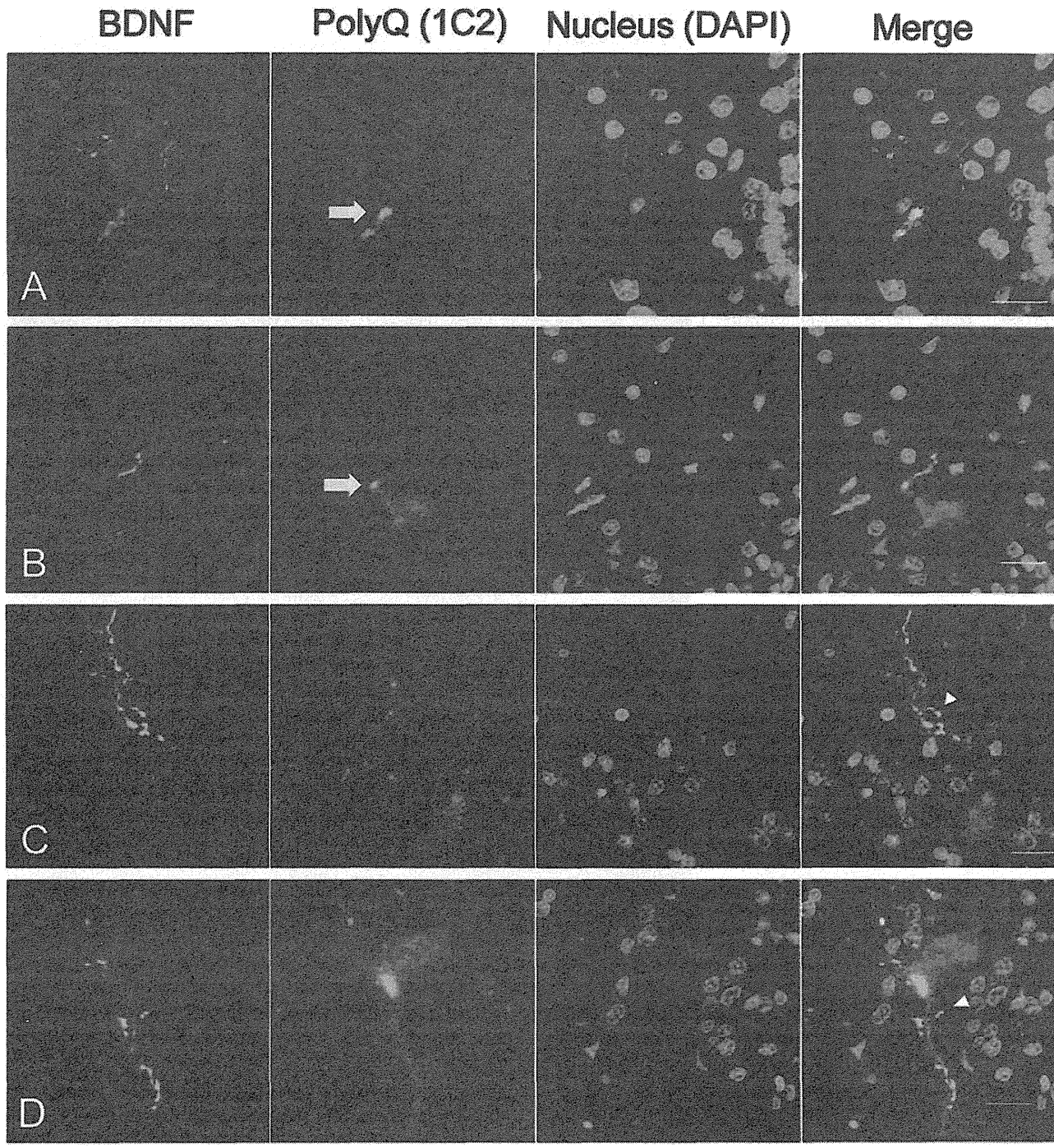

Fig. 3 The brain-derived neurotrophic factor (BDNF)-immunoreactive granules are observed in the vicinity of α1A voltage-dependent calcium channel protein ($Ca_v2.1$) aggregates. Double immunofluorescence with 1C2 antibody and anti-BDNF antibody in spinocerebellar ataxia type 6 (SCA6) patient cerebella. (A, B) 1C2-positive polyglutamine (polyQ) aggregates often existed in the proximal portion of dendrites, such as the primary shaft (A; arrow) or the secondary shaft (B; arrow), of Purkinje cells. BDNF-immunoreactive structures were seen distal to the 1C2-positive polyQ aggregates (A, B). (C, D) BDNF-immunoreactive granules were seen not only within the contour of Purkinje cell dendrites, but also outside the visible dendritic structures (arrow head). (For A–D: scale bars: 20 μm).

reduction of BDNF gene expression is due to reduced amounts of CREB in the nuclei by sequestration of CREB in the cytoplasm by $Ca_v2.1$ aggregates. Further studies are needed to elucidate how the cytoplasmic aggregates cause the suppression of CREB-target transcription.

The other key finding in the present study is that there are abundant BDNF-immunoreactive granules, mainly in the dendrites of SCA6 Purkinje cells. Previous studies indicate that these BDNF-immunoreactive granules are not stained by ubiquitin antibodies, since SCA6 lacks ubiquitin-positive structures.[4,26] As far as we have investigated in five SCA6 cerebellar specimens, the BDNF-immunoreactive granules were restricted to the Purkinje cells, similar to the $Ca_v2.1$ aggregates. For example, we did not observe any BDNF aggregates in the cerebellar granule cells or in the neurons of the dentate nucleus. Further studies using larger numbers of SCA6 patients would be important to address whether the BDNF granules are also seen in other SCA6 brain regions. Although we observed many BDNF-immunoreactive granules within dendrites under light microscopy, we also suspected that some of these granules appear to exist outside the dendritic contour. It may be possible that they are still inside the small dendritic sprouts, which were only invisible due to degeneration. Alternatively, they may have been secreted from the dendrites as previously postulated.[27] Precise investigation using electron microscopes is needed.

Previous studies investigating the BDNF immunohistochemistry in adult rat, guinea pig and Japanese macaque cerebella have shown that BDNF is expressed diffusely in the cell body and the dendrites of Purkinje cells.[20,28,29] One previous study describes granular BDNF immunoreactivity in the control human Purkinje cell dendrites, although detailed information is not available.[30] In the present study, we observed that BDNF immunoreactivity was very weak in human post mortem control specimens. This discrepancy in the immunostaining intensities between previous studies and the present one may be due to differences in tissue preparation, such as fixation: paraformaldehyde[12] or paraformaldehyde with picric acid[26] may be more suitable fixations for BDNF immunohistochemistry than the formalin we employed. Nevertheless, the granular BDNF-immunoreactive granules in Purkinje cells were specific to SCA6 in the present cohort, indicating that this finding is meaningful.

It is remains unclear how BDNF-immunoractive granules are formed in SCA6 Purkinje cells. The BDNF protein, still translated from reduced BDNF mRNA, needs to be subjected to many processes, such as post-translational modification and needs to be transported in cells to become functional. As we observed 1C2-immunoreactive $Ca_v2.1$ aggregates in the proximal portion of the dendrites, such as the primary shaft, it is tempting to speculate that BDNF trafficking in the dendrites may be disturbed, resulting in the formation of visible BDNF-immunoreactive granules in dendrites of SCA6 Purkinje cells. The $Ca_v2.1$ aggregates, shown by A6RPT-#5803 immunohistochemistry (Fig. 2g), were seen in the cell body through distal dendrites, suggesting that the $Ca_v2.1$ aggregates widely prevail in the somato-dendritic cytoplasm. The BDNF normally moves in the dendrites in both directions (antero- and retro-grade transports) between the post-synaptic button and cell body,[31] as well as from the cell body to the presynaptic terminal through anterograde axonal transport. Therefore, it may be possible that $Ca_v2.1$ aggregates disturbed BDNF trafficking in the dendrites. Interestingly, SCA2, which also forms polyQ aggregates in the cytoplasm of Purkinje cells (Fig. 2c), did not show similar BDNF-immunoreactive granules in the dendrites of Purkinje cells. Therefore, it may be possible that a certain factor specific to $Ca_v2.1$ may underlie formation of BDNF-positive granules. For example, the secretion of BDNF from dendrites (post-synaptic secretion) is considered regulated by intracellular Ca^{2+} concentration, which is in turn regulated by *N*-methyl-D-aspartate receptors, inositol tri-phosphate receptor (IP3R) and voltage-dependent calcium channels including $Ca_v2.1$.[32] Further studies are needed to address how $Ca_v2.1$ formation leads to BDNF-immunoreactive granules in the dendrites.

In conclusion, the decrease of BDNF gene expression level and abnormal BDNF-immunoreactive granules were seen in SCA6 cerebellum. Precise understanding of the implication of altered gene expressions, including BDNF, and of the mechanism generating BDNF-immunoreactive granules, may be important for establishing fundamental therapies for SCA6.

ACKNOWLEDGMENTS

This study was funded by the Japanese Ministry of Education, Sports and Culture (KI and HM), the Japan Society for Promotion of Science (JSPS) (KI and HM), the 21st Century COE Program on Brain Integration and its Disorders from the Japanese Ministry of Education, Science and Culture (HM), the Strategic Research Program for Brain Sciences by the Ministry of Education, Culture, Sports, Science and Technology of Japan (HM), Core Research for Evolutional Science and Technology (CREST), Japan Science and Technology Agency (JST), Saitama, Japan (HM), from the Health and Labour Sciences Research Grants on Ataxic Diseases (HM) of the Japanese Ministry of Health, Labour and Welfare, Japan, and by a Grant-in-Aid for Scientific Research on Innovative Areas (Comprehensive Brain Science Network) from the Ministry of Education, Science, Sports and Culture of Japan (SM).

The authors thank Mr. Noboru Ando and Mrs. Hitomi Matsuo (Tokyo Medical and Dental University) for their excellent technical assistance.

AUTHOR CONTRIBUTIONS

M. Takahashi, the first author, performed research, analyzed data and wrote the manuscript, while four others (NS, MO, YN and TI) partly performed research, and seven others (MY, HT, TK, OM, M. Takao, SM and YE) performed neuropathological examinations and assisted pathological analysis of this study, HM organized and arranged the whole project and KI designed, directed and wrote this work.

REFERENCES

1. Ishikawa K, Tanaka H, Saito M *et al.* Japanese families with autosomal dominant pure cerebellar ataxia map to chromosome 19p13.1-p13.2 and are strongly associated with mild CAG expansions in the spinocerebellar ataxia type 6 gene in chromosome 19p13.1. *Am J Hum Genet* 1997; **61**: 336–346.
2. Gomez CM, Thompson RM, Gammack JT *et al.* Spinocerebellar ataxia type 6: gaze-evoked and vertical nystagmus, Purkinje cell degeneration, and variable age of onset. *Ann Neurol* 1997; **42**: 933–950.
3. Zhuchenko O, Bailey J, Bonnen P *et al.* Autosomal dominant cerebellar ataxia (SCA6) associated with small polyglutamine expansions in the alpha 1A-voltage-dependent calcium channel. *Nat Genet* 1997; **15**: 62–69.
4. Ishikawa K, Fujigasaki H, Saegusa H *et al.* Abundant expression and cytoplasmic aggregations of [alpha]1A voltage-dependent calcium channel protein associated with neurodegeneration in spinocerebellar ataxia type 6. *Hum Mol Genet* 1999; **8**: 1185–1193.
5. Ishikawa K, Owada K, Ishida K *et al.* Cytoplasmic and nuclear polyglutamine aggregates in SCA6 Purkinje cells. *Neurology* 2001; **56**: 1753–1756.
6. Yabe I, Sasaki H, Matsuura T *et al.* SCA6 mutation analysis in a large cohort of the Japanese patients with late-onset pure cerebellar ataxia. *J Neurol Sci* 1998; **156**: 89–95.
7. Takahashi H, Ishikawa K, Tsutsumi T *et al.* A clinical and genetic study in a large cohort of patients with spinocerebellar ataxia type 6. *J Hum Genet* 2004; **49**: 256–264.
8. Orr HT, Zoghbi HY. Trinucleotide repeat disorders. *Annu Rev Neurosci* 2007; **30**: 575–621.
9. DiFiglia M, Sapp E, Chase KO *et al.* Aggregation of huntingtin in neuronal intranuclear inclusions and dystrophic neurites in brain. *Science* 1997; **277**: 1990–1993.
10. Paulson HL, Perez MK, Trottier Y *et al.* Intranuclear inclusions of expanded polyglutamine protein in spinocerebellar ataxia type 3. *Neuron* 1997; **19**: 333–344.
11. Binder DK, Scharfman HE. Brain-derived neurotrophic factor. *Growth Factors* 2004; **22**: 123–131.
12. Ferrer I, Goutan E, Marin C, Rey MJ, Ribalta T. Brain-derived neurotrophic factor in Huntington disease. *Brain Res* 2000; **866**: 257–261.
13. Zuccato C, Cattaneo E. Role of brain-derived neurotrophic factor in Huntington's disease. *Prog Neurobiol* 2007; **81**: 294–330.
14. Zuccato C, Ciammola A, Rigamonti D *et al.* Loss of huntingtin-mediated BDNF gene transcription in Huntington's disease. *Science* 2001; **293**: 493–498.
15. Gharami K, Xie Y, An JJ, Tonegawa S, Xu B. Brain-derived neurotrophic factor over-expression in the forebrain ameliorates Huntington's disease phenotypes in mice. *J Neurochem* 2008; **105**: 369–379.
16. Steffan JS, Kazantsev A, Spasic-Boskovic O *et al.* The Huntington's disease protein interacts with p53 and CREB-binding protein and represses transcription. *Proc Natl Acad Sci USA* 2000; **97**: 6763–6768.
17. Nucifora FC, Jr, Sasaki M, Peters MF *et al.* Interference by huntingtin and atrophin-1 with cbp-mediated transcription leading to cellular toxicity. *Science* 2001; **291**: 2423–2428.
18. McCampbell A, Taylor JP, Taye AA *et al.* CREB-binding protein sequestration by expanded polyglutamine. *Hum Mol Genet* 2000; **9**: 2197–2202.
19. Ishiguro T, Ishikawa K, Takahashi M *et al.* The carboxy-terminal fragment of alpha(1A) calcium channel preferentially aggregates in the cytoplasm of human spinocerebellar ataxia type 6 Purkinje cells. *Acta Neuropathol* 2010; **119**: 447–464.
20. Dieni S, Rees S. Distribution of brain-derived neurotrophic factor and TrkB receptor proteins in the fetal and postnatal hippocampus and cerebellum of the guinea pig. *J Comp Neurol* 2002; **454**: 229–240.
21. Gauthier LR, Charrin BC, Borrell-Pages M *et al.* Huntingtin controls neurotrophic support and survival of neurons by enhancing BDNF vesicular transport along microtubules. *Cell* 2004; **118**: 127–138.
22. Miyashita T, Tabuchi A, Fukuchi M *et al.* Interference with activity-dependent transcriptional activation of BDNF gene depending upon the expanded polyglutamines in neurons. *Biochem Biophys Res Commun* 2005; **333**: 1241–1248.
23. Hourez R, Servais L, Orduz D *et al.* Aminopyridines correct early dysfunction and delay neurodegeneration in a mouse model of spinocerebellar ataxia type 1. *J Neurosci* 2011; **31**: 11795–11807.

24. Schindowski K, Belarbi K, Buee L. Neurotrophic factors in Alzheimer's disease: role of axonal transport. *Genes Brain Behav* 2008; **7** (Suppl 1): 43–56.
25. Howells DW, Porritt MJ, Wong JY *et al.* Reduced BDNF mRNA expression in the Parkinson's disease substantia nigra. *Exp Neurol* 2000; **166**: 127–135.
26. Ishikawa K, Watanabe M, Yoshizawa K *et al.* Clinical, neuropathological, and molecular study in two families with spinocerebellar ataxia type 6 (SCA6). *J Neurol Neurosurg Psychiatry* 1999; **67**: 86–89.
27. Matsuda N, Lu H, Fukata Y *et al.* Differential activity-dependent secretion of brain-derived neurotrophic factor from axon and dendrite. *J Neurosci* 2009; **29**: 14185–14198.
28. Kawamoto Y, Nakamura S, Nakano S, Oka N, Akiguchi I, Kimura J. Immunohistochemical localization of brain-derived neurotrophic factor in adult rat brain. *Neuroscience* 1996; **74**: 1209–1226.
29. Kawamoto Y, Nakamura S, Kawamata T, Akiguchi I, Kimura J. Cellular localization of brain-derived neurotrophic factor-like immunoreactivity in adult monkey brain. *Brain Res* 1999; **821**: 341–349.
30. Murer MG, Boissiere F, Yan Q *et al.* An immunohistochemical study of the distribution of brain-derived neurotrophic factor in the adult human brain, with particular reference to Alzheimer's disease. *Neuroscience* 1999; **88**: 1015–1032.
31. Adachi N, Kohara K, Tsumoto T. Difference in trafficking of brain-derived neurotrophic factor between axons and dendrites of cortical neurons, revealed by live-cell imaging. *BMC Neurosci* 2005; **6**: 42.
32. Kuczewski N, Porcher C, Lessmann V, Medina I, Gaiarsa JL. Activity-dependent dendritic release of BDNF and biological consequences. *Mol Neurobiol* 2009; **39**: 37–49.

Neurobiology of Aging 34 (2013) 1101–1104

Contents lists available at SciVerse ScienceDirect

Neurobiology of Aging

journal homepage: www.elsevier.com/locate/neuaging

Brief communication

Suspected limited efficacy of γ-secretase modulators

Nobuto Kakuda [a,b], Kohei Akazawa [c], Hiroyuki Hatsuta [d], Shigeo Murayama [d], Yasuo Ihara [a,b,e,f,*], The Japanese Alzheimer's Disease Neuroimaging Initiative

[a] Department of Neuropathology, Faculty of Life and Medical Sciences, Doshisha University, Kyoto, Japan
[b] Core Research for Evolutional Science and Technology (CREST), Japan Science and Technology Agency, Saitama, Japan
[c] Department of Medical Informatics, Niigata University Medical and Dental Hospital, Niigata University, Niigata, Japan
[d] Department of Neuropathology, Tokyo Metropolitan Institute of Gerontology, Tokyo, Japan
[e] Center for Neurologic Diseases, Doshisha University, Kyoto, Japan
[f] New Energy and Industrial Technology Development Organization (NEDO), Kanagawa, Japan

ARTICLE INFO

Article history:
Received 16 June 2012
Accepted 25 August 2012
Available online 9 October 2012

Keywords:
γ-Secretase
γ-Modulator
Alzheimer's disease

ABSTRACT

Mild cognitive impairment and Alzheimer's disease (AD) are associated with changes in γ-secretase activity in the brain, producing an amyloid β-protein-42-lowering γ-modulator-like effect. We show here that this modulation occurs at the stage of amyloid deposition, presumably decades earlier than the onset of AD. In addition, γ-secretase modulator-1, a γ-modulator, altered γ-secretase activity in the AD brain but to a lesser extent than in the normal brain. These findings suggest that γ-modulators have limited efficacy against amyloid deposition and AD.

1. Introduction

Amyloid β-protein (Aβ) is cleaved sequentially from amyloid precursor protein by β- and γ-secretases (for a review see Selkoe, 2001). The longer but minor species, Aβ42, predominates in senile plaques (Iwatsubo et al., 1994). γ-Secretase, a heterogeneous complex (Takasugi et al., 2003; Serneels et al., 2009), governs the intramembrane proteolysis of type I membrane proteins including amyloid precursor protein (Sisodia and St George-Hyslop, 2002; Wakabayashi and De Strooper, 2008). We found recently that γ-secretase activity is altered in brains affected by mild cognitive impairment (MCI) or Alzheimer's disease (AD). The change decreases the concentrations of both Aβ42 and Aβ43 in cerebrospinal fluid (CSF) in patients affected with MCI or AD. To compensate for these decreases, the levels of Aβ38 and Aβ40 are increased (Kakuda et al., 2012). We assume that Aβ42 and Aβ43 are enhanced to be converted by stepwise processing to Aβ38 and Aβ40, respectively, by altered γ-secretase in the brain affected by MCI or AD (Kakuda et al., 2012; Takami et al., 2009). Reciprocal changes in the levels of Aβ42 and Aβ38 without a change in the total Aβ level are an essential characteristic of γ-secretase modulators, drugs whose development receives intense attention.

2. Materials and methods

2.1. Subjects

Human cortical specimens for quantification of raft-associated γ-secretase activity were obtained from brains that had been removed, processed, and stored at −80 °C within 12 hours postmortem; the bodies had been placed in a cold (4 °C) room within 2 hours after death. The specimens were kept at the Brain Bank at Tokyo Metropolitan Institute of Gerontology. For all the brains registered at the bank we obtained written informed consent for their use for medical research from the patient or the patient's family. Each brain specimen (approximately 0.5 g) was taken from Brodmann areas 9–11 of 13 AD patients (80 ± 5.0 years of age; Braak neurofibrillary tangle [NFT] stage >IV; senile plaque [SP] stage = C; retrospective clinical dementia rating [CDR] >1), 10 SP stage B patients (76 ± 4.0 years of age; Braak NFT stage >I; retrospective CDR = 0), 10 SP stage A patients (76 ± 4.7 years of age; Braak NFT stage >0; retrospective CDR = 0), and 16 controls in SP stage 0 (77 ± 6.5 years of age; Braak NFT stage <I; retrospective CDR = 0). SP stages were determined by modified methenamine silver stain: stage A: Aβ deposits in the basal portions of the isocortex; stage B: Aβ deposits in virtually all isocortical association

* Corresponding author at: Department of Neuropathology, Faculty of Life and Medical Sciences, Doshisha University, 4-1-1, Kizugawadai, Kizugawa, Kyoto 619-0225, Japan. Tel.: +81 774 65 6058; fax: +81 3 5800 6852.
E-mail address: yihara@mail.doshisha.ac.jp (Y. Ihara).

0197-4580/$ – see front matter © 2013 Elsevier Inc. All rights reserved.
http://dx.doi.org/10.1016/j.neurobiolaging.2012.08.017

areas except primary centers; stage C (AD): Aβ deposits in all areas of the isocortex including primary motor and sensory centers (Braak and Braak, 1991).

2.2. Quantification of brain raft-associated γ-secretase activity

A previously reported assay method was employed with some modifications (Kakuda et al., 2012). Briefly, each raft fraction, adjusted to 100 μg/mL in protein concentration, was incubated with 200 nM of βCTF-FLAG for 1 hour at 37 °C in the presence of 0, or 0.1–0.5 μM γ-secretase modulator (GSM)-1 (kindly provided by Dr M. Okochi, Osaka University). After incubation, all samples were centrifuged at 265,000g on a TLA110 rotor (Beckman, Palo Alto, CA, USA) for 20 minutes at 4 °C. The supernatants were separated on sodium dodecyl sulfate polyacylamide gel electrophoresis (SDS-PAGE), and subjected to quantitative Western blot analysis, using specific antibodies, 3B1 for Aβ38, BA27 for Aβ40, 44A3 for Aβ42, and anti-Aβ43 polyclonal for Aβ43.

2.3. GSM-1-induced shift of ln(Aβ38/42)

Shifts of ln(Aβ38/42) with GSM-1 were calculated as GSM-1-induced ln(Aβ38/42) minus the ratio measured in its absence.

2.4. Statistical analysis

All statistical analyses were performed using SPSS version 14.0. Data transformation was required to achieve normal distributions; all analyses were performed after logarithmic transformation of the data for Aβ38, Aβ40, Aβ42, and Aβ43. Analysis of variance was used to test the equality of mean values for continuous variables between the 4 groups: control, SP stage A, SP stage B, and AD. Multiple comparisons were made using Bonferroni *t* test to test the differences between controls, SP stage A, SP stage B, and AD. The paired *t* test was used to examine the effect of GSM-1 treatment. *p* values <0.05 were considered significant.

3. Results

We speculated that this modulation in the γ-secretase activity occurs much earlier than the onset of AD because lower Aβ42 concentrations in CSF appear to be associated with amyloid deposition itself (Fagan et al., 2006). To confirm this, we measured the activities of raft-associated γ-secretase prepared from autopsied brains using a previously established method (Kakuda et al., 2012). Raft fractions were prepared from control and AD brains (Brodmann areas 9–11), which were judged histochemically to be in the Braak SP stage 0, stage A, stage B, or stage C (AD) (Braak and Braak, 1991). Aβs produced by γ-secretase from each brain specimen were analyzed by quantitative Western blot, and the ln(Aβ40/43) and ln(Aβ38/42) ratios were obtained. Stage A plots nearly superimposed with control plots (Fig. 1; 0 vs. A: $p = 1.000$ for ln(Aβ40/43), $p = 1.000$ for ln(Aβ38/42)). However, the γ-secretase activities differed between stage B specimens and 0/A specimens (0 vs. B: $p = 0.005$ for ln(Aβ40/43) and $p < 0.001$ for ln(Aβ38/42); A vs. B: $p = 0.002$ for ln(Aβ40/43) and $p = 0.001$ for ln(Aβ38/42); Fig. 1). AD (stage C) plots were shifted the most (0 vs. C: $p < 0.001$ for ln(Aβ40/43) and $p = 0.003$ for ln(Aβ38/42); A vs. C: $p < 0.001$ for ln(Aβ40/43) and $p = 0.007$ for ln(Aβ38/42)). Most interestingly, although AD plots were shifted to the same extent as stage B plots for Aβ38/42 (B vs. C: $p = 1.000$ for ln(Aβ38/42)), stage B and AD plots differ for Aβ40/43 (B vs. C: $p < 0.001$ for ln(Aβ40/43); Fig. 1).

Although these data were obtained from a cross-sectional study, one might assume that stage A develops through to stage B and eventually to stage C over decades (Duyckaerts and Hauw, 1997).

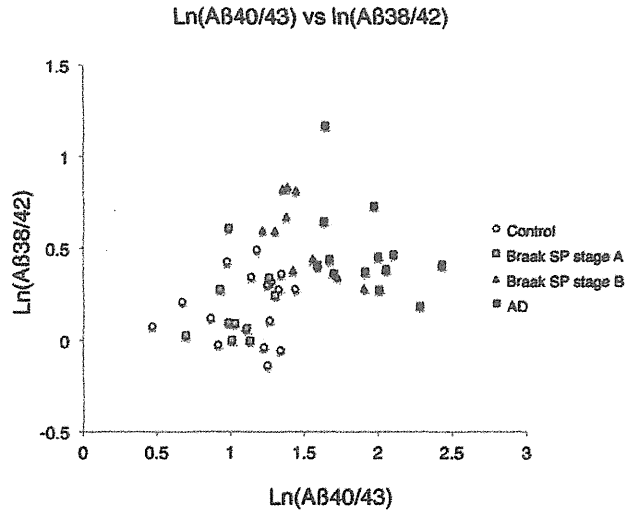

Fig. 1. Ln(amyloid-β protein [Aβ]40/43) versus ln(Aβ38/42) plot of raft-associated γ-secretase prepared from the brains in various (Braak) senile plaque (SP) stages. The raft-associated γ-secretase prepared from Braak SP stages 0, A, B, and C (AD) brain specimens were incubated with 200 nM of βCTF for 1 hour at 37 °C. After centrifugation of the reaction mixtures, the supernatants were saved for quantitative Western blot analysis of Aβs using specific antibodies.

Thus, the Aβ42 product line of γ-secretase appears to undergo changes early and the Aβ42-lowering activity remains constant through to development of AD. By contrast, the Aβ40 product line gradually changes with increasing Aβ40/43 ratio, as stage 0/A develops to stage B and finally to AD. Our previous observations showed that Aβ42 levels in CSF parallel the Aβ38/42 ratio, and Aβ43 levels parallel the Aβ40/43 ratio (Kakuda et al., 2012). These findings suggest that a decrease in the Aβ42 level would be the first alteration observable in CSF and that the level does not change throughout the disease course, whereas the Aβ43 level in CSF would decrease progressively up to AD.

We noted previously that the effects of Aβ42-lowering γ-modulators could be minimal in sporadic MCI/AD patients because modulation of γ-secretase has already begun in their brains. As mentioned above, the modulation of γ-secretase is evident in stage B. Accordingly, we investigated the response of γ-secretase to GSM-1, an Aβ42-lowering modulator, in control and AD brains. We reasoned that a strong response of the altered γ-secretase to GSM-1 would indicate that the drug might still be effective.

We quantified γ-secretase activities in the absence or presence of GSM-1 in control and AD specimens. This agent is known to aggressively modulate only conversion from Aβ42 to Aβ38, but not that from Aβ43 to Aβ40 (Crump et al., 2011; Ebke et al., 2011; Ohki et al., 2011). As expected, GSM-1 treatment significantly lowered Aβ42 and increased Aβ38 in control (see Supplementary Fig. 1). By contrast, in AD specimens, GSM-1 lowered Aβ42 and increased Aβ38 but to a lesser extent (Supplementary Fig. 1). The generation of Aβ40 and Aβ43, and the total production of Aβ were unchanged by the treatment of GSM-1 in all specimens (Supplementary Fig. 1).

In AD specimens, conversion of Aβ43 to Aβ40 seems to be altered compared with control (Kakuda et al., 2012), but this might be due to high concentrations of GSM-1 (>0.5 μM), which suppressed Aβ40 (and Aβ43) product line and total Aβ production in both control and AD specimens (data not shown). GSM-1 treatment significantly elevated the ratio of Aβ38/42 in control (Aβ38/42 with dimethyl sulfoxide vs. Aβ38/42 with GSM-1; $p < 0.000$, paired *t* test; Fig. 2A). By contrast, the same treatment of AD specimens

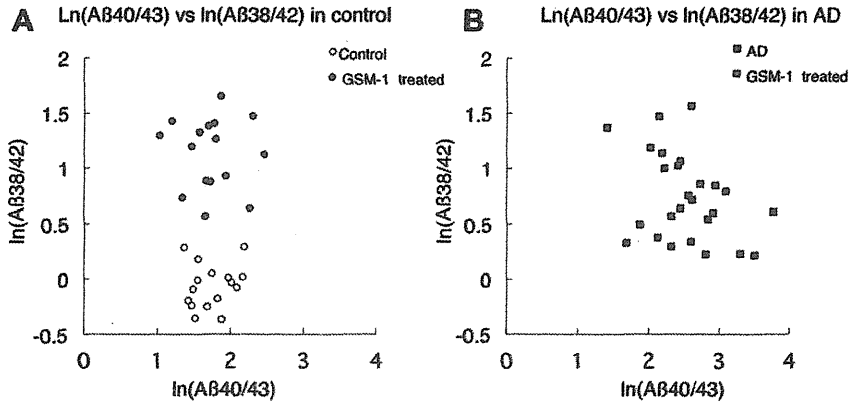

Fig. 2. Ln(amyloid-β protein [Aβ]40/43) versus ln(Aβ38/42) plot of γ-secretase modulator (GSM)-1-treated raft-associated γ-secretase activity. The raft-associated γ-secretases prepared from control (A) and AD (B) brains were incubated with 200 nM of βCTF for 1 hour at 37 °C in the presence of dimethyl sulfoxide or 0.3 μM GSM-1. Aβs produced were quantified by quantitative Western blot analysis using specific antibodies.

caused a much smaller increase in the Aβ38/42 ratio ($p < 0.001$ for AD paired t test; Fig. 2B). There was no significant difference in the Aβ40/43 ratio between control and AD specimens (Aβ40/43 with dimethyl sulfoxide vs. Aβ40/43 with GSM-1; $p = 0.814$ for control; $p = 0.223$ for AD, respectively; paired t test; Fig. 2A and B). The modulating effect on the Aβ38/42 ratio can be interpreted as indicating the extent of GSM-1-induced shift in the Aβ38/42 ratio (Supplementary Table 1). γ-Secretase was associated with significantly lower ratios in AD specimens than in control specimens (control vs. AD: $p < 0.001$), indicating a poor response to GSM-1 in AD specimens.

4. Discussion

Modulation of γ-secretase occurs in AD brains (Kakuda et al., 2012), and to a significant extent already at the stage of amyloid deposition, a decade or even decades before the onset of AD (Duyckaerts and Hauw, 1997). Although γ-secretase self-modulates and produces less Aβ42, it is likely that β-amyloid accumulation slowly progresses and ultimately extends throughout the brain, finally involving primary cortical centers (Duyckaerts and Hauw, 1997). A gradual decline in the rate of Aβ accumulation curve (Kawarabayashi et al., 2001) might be caused by self-modulation of γ-secretase. Currently, we do not know which comes first, Aβ deposition or γ-self-modulation. However, the efficacy of GSM-1 and γ-modulators in general would be limited when Aβ42 deposition and self-modulation of γ-secretase begins in the brain. To date, the efficacy of γ-modulators has been confirmed most often using younger Tg2576 mice, which do not yet accumulate Aβ (Borgegard et al., 2012; Kounnas et al., 2010). In Tg2576 mice, Aβ deposition starts at 9–12 months, and γ-secretase activity changes together with increasing Aβ deposition in the brain starting at 15–16 months of age (Kawarabayashi et al., 2001; data not shown). Thus, the true effectiveness of γ-modulators in Tg2576 mice should be assessed after 15–16 months of age. It is unclear whether γ-modulators are effective in such amyloid-bearing aged mice.

Disclosure statement

The authors have no conflict of interest.

Ethic permission was approved by Faculty of Life and Medical Sciences, Doshisha University, and we obtained written informed consent for their use for medical research from the patient or the patient's family.

Acknowledgements

The authors thank Dr Masayasu Okochi, Neuropsychiatry and Neurochemistry, Department of Integrated Medicine, Osaka University Graduate School of Medicine, for kindly providing GSM-1, and Dr Satoru Funamoto, Department of Neuropathology, Faculty of Life and Medical Sciences, Doshisha University, for providing βCTF. This project was supported in part by the New Energy and Industrial Technology Development Organization, Japan (J-ADNI) and by the MEXT-Supported Program for the Strategic Research Foundation at Private Universities, 2012–2017.

Appendix A. Supplementary data

Supplementary data associated with this article can be found, in the online version, at http://dx.doi.org/10.1016/j.neurobiolaging.2012.08.017.

References

Borgegard, T., Juréus, A., Olsson, F., Rosqvist, S., Sabirsh, A., Rotticci, D., Paulsen, K., Klintenberg, R., Yan, H., Waldman, M., Stromberg, K., Nord, J., Johansson, J., Regner, A., Parpal, S., Malinowsky, D., Radesater, A.C., Li, T., Singh, R., Eriksson, H., Lundkvist, J., 2012. First and second generation γ-secretase modulators (GSMs) modulate amyloid-β (Aβ) peptide production through different mechanisms. J. Biol. Chem. 287, 11810–11819.

Braak, H., Braak, E., 1991. Neuropathological stageing of Alzheimer-related changes. Acta Neuropathol. 82, 239–259.

Crump, C.J., Fish, B.A., Castro, S.V., Chau, D.M., Gertsik, N., Ahn, K., Stiff, C., Pozdnyakov, N., Bales, K.R., Johnson, D.S., Li, Y.M., 2011. Piperidine acetic acid based γ-secretase modulators directly bind to Presenilin-1. ACS Chem. Neurosci. 2, 705–710.

Duyckaerts, C., Hauw, J.J., 1997. Prevalence, incidence and duration of Braak's stages in the general population: can we know? Neurobiol. Aging 18, 362–369.

Ebke, A., Luebbers, T., Fukumori, A., Shirotani, K., Haass, C., Baumann, K., Steiner, H., 2011. Novel γ-secretase enzyme modulators directly target presenilin protein. J. Biol. Chem. 286, 37181–37186.

Fagan, A.M., Mintun, M.A., Mach, R.H., Lee, S.Y., Dence, C.S., Shah, A.R., LaRossa, G.N., Spinner, M.L., Klunk, W.E., Mathis, C.A., DeKosky, S.T., Morris, J.C., Holtzman, D.M., 2006. Inverse relation between in vivo amyloid imaging load and cerebrospinal fluid Abeta42 in humans. Ann. Neurol. 59, 512–519.

Iwatsubo, T., Odaka, A., Suzuki, N., Mizusawa, H., Nukina, N., Ihara, Y., 1994. Visualization of Aβ42(43) and Aβ40 in senile plaque with end-specific Aβ monoclonals: evidence that an initially deposited forms is Aβ42(43). Neuron 13, 45–53.

Kakuda, N., Shoji, M., Arai, H., Furukawa, K., Ikeuchi, T., Akazawa, K., Takami, M., Hatsuta, H., Murayama, S., Hashimoto, Y., Miyajima, M., Arai, H., Nagashima, Y., Yamaguchi, H., Kuwano, R., Nagaike, K., Ihara, Y., Japanese Alzheimer's Disease Neuroimaging Initiative, 2012. Altered γ-secretase activity in mild cognitive impairment and Alzheimer's disease. EMBO Mol. Med. 4, 344–352.

Kawarabayashi, T., Younkin, L.H., Saido, T.C., Shoji, M., Ashe, K.H., Younkin, S.G., 2001. Age-dependent changes in brain, CSF, and plasma amyloid (β) protein in the Tg2576 transgenic mouse model of Alzheimer's disease. J. Neurosci. 21, 372–381.

Kounnas, M.Z., Danks, A.M., Cheng, S., Tyree, C., Ackerman, E., Zhang, X., Ahn, K., Nguyen, P., Comer, D., Mao, L., Yu, C., Pleynet, D., Digregorio, P.J., Velicelebi, G., Stauderman, K.A., Comer, W.T., Mobley, W.C., Li, Y.M., Sisodia, S.S., Tanzi, R.E., Wagner, S.L., 2010. Modulation of gamma-secretase reduces beta-amyloid deposition in a transgenic mouse model of Alzheimer's disease. Neuron 67, 769–780.

Ohki, Y., Higo, T., Uemura, K., Shimada, N., Osawa, S., Berezovska, O., Yokoshima, S., Fukuyama, T., Tomita, T., Iwatsubo, T., 2011. Phenylpiperidine-type γ-secretase modulators target the transmembrane domain 1 of presenilin 1. EMBO J. 30, 4815–4824.

Selkoe, D.J., 2001. Alzheimer's disease: genes, proteins, and therapy. Physiol. Rev. 81, 741–766.

Serneels, L., Van Biervliet, J., Craessaerts, K., Dejaegere, T., Horré, K., Van Houtvin, T., Esselmann, H., Paul, S., Schäfer, M.K., Berezovska, O., Hyman, B.T., Sprangers, B., Sciot, R., Moons, L., Jucker, M., Yang, Z., May, P.C., Karran, E., Wiltfang, J., D'Hooge, R., De Strooper, B., 2009. γ-Secretase heterogeneity in the Aph1 subunit: relevance for Alzheimer's disease. Science 324, 639–642.

Sisodia, S.S., St George-Hyslop, P.H., 2002. gamma-Secretase, Notch, Abeta and Alzheimer's disease: where do the presenilins fit in? Nat. Rev. Neurosci. 3, 281–290.

Takami, M., Nagashima, Y., Sano, Y., Ishihara, S., Morishima-Kawashima, M., Funamoto, S., Ihara, Y., 2009. γ-Secretase: successive tripeptide and tetrapeptide release from the transmembrane domain of β-carboxyl terminal fragment. J. Neurosci. 29, 13042–13052.

Takasugi, N., Tomita, T., Hayashi, I., Tsuruoka, M., Niimura, M., Takahashi, Y., Thinakaran, G., Iwatsubo, T., 2003. The role of presenilin cofactors in the γ-secretase complex. Nature 422, 438–441.

Wakabayashi, T., De Strooper, B., 2008. Presenilins: members of the gamma-secretase quartets, but part-time soloists too. J. Physiol. 23, 194–204.

NEUROPATHOLOGY

Neuropathology 2012; ••, ••–••

doi:10.1111/j.1440-1789.2012.01329.x

Original Article

Neuropathologic analysis of Lewy-related α-synucleinopathy in olfactory mucosa

Sayaka Funabe,[1,4] Masaki Takao,[1] Yuko Saito,[5] Hiroyuki Hatsuta,[1] Mikiko Sugiyama,[1] Shinji Ito,[1] Kazutomi Kanemaru,[2] Motoji Sawabe,[3] Tomio Arai,[3] Hideki Mochizuki,[6] Nobutaka Hattori[4] and Shigeo Murayama[1]

Departments of [1]Neuropathology, [2]Neurology, [3]Pathology, Tokyo Metropolitan Geriatric Hospital and Institute of Gerontology, [4]Department of Neurology, Juntendo University, [5]Department of Laboratory Medicine, National Center Hospital for Neurology and Psychiatry, Tokyo and [6]Department of Neurology, Faculty of Medicine, Osaka University, Osaka, Japan

We analyzed the incidence and extent of Lewy-related α-synucleinopathy (LBAS) in the olfactory mucosa, as well as the central and peripheral nervous systems of consecutive autopsy cases from a general geriatric hospital. The brain and olfactory mucosa were immunohistochemically examined using antibodies raised against phosphorylated α-synuclein. Thirty-nine out of 105 patients (37.1%) showed LBAS in the central or peripheral nervous systems. Seven patients presented LBAS (Lewy neurites) in the olfactory lamina propria mucosa. One out of the seven cases also showed a Lewy neurite in a bundle of axons in the cribriform plate, but α-synuclein deposits were not detected in the olfactory receptor neurons. In particular, high incidence of α-synuclein immunopositive LBAS in the olfactory mucosa was present in the individuals with clinically as well as neuropathologically confirmed Parkinson's disease and dementia with Lewy bodies (6/8 cases, 75%). However, this pathologic alteration was rare in the cases with incidental or subclinical Lewy body diseases (LBD) (one out of 31 cases, 3.2%). In the olfactory bulb, the LBAS was usually present in the glomeruli and granular cells of most symptomatic and asymptomatic cases with LBD. Our studies further confirmed importance of the olfactory entry zone in propagation of LBAS in the human aging nervous system.

Key words: α-synuclein, Lewy body, neuropathology, olfactory mucosa, Parkinson's disease.

INTRODUCTION

Sporadic Parkinson's disease is a neurodegenerative disorder characterized clinically by resting tremor, rigidity, bradykinesia and gait disturbance, as well as neuropathologically by the loss of neurons in several brainstem nuclei and the presence of Lewy bodies formed by abnormal accumulation of α-synuclein.[1–5] Of the many types of neurons in the central and peripheral nervous systems, a specific subset of neurons is vulnerable to accumulation of α-synuclein, which takes the form of aggregates such as Lewy bodies and Lewy neurites (LBs/LNs).[6–8]

Based on studies of a large number of autopsy cases, the initial sites involved in Lewy-related pathology are reported to be the dorsal motor nucleus of the vagus, the intermediate reticular zone in the lower brainstem and olfactory bulb.[9,10] We previously reported that in the earliest stage of Lewy-related α-synucleinopathy (LBAS), abnormal α-synuclein accumulation extends from the peripheral part of the olfactory bulb to the anterior olfactory nucleus as well as the amygdala.[11] From a clinical standpoint, impaired olfactory function constitutes one of the earliest symptoms of sporadic Parkinson's disease.[12,13] Therefore, the olfactory system may be one of the vital regions in the development of Lewy body disease (LBD).

In the olfactory bulb, α-synuclein accumulation is observed in the anterior olfactory nucleus as well as the mitral, tufted, and granular cells of individuals with clinical Parkinson's disease or dementia with Lewy bodies (DLB). Even in the early stages of these diseases, LNs, LBs or both, can be seen in the olfactory bulbs.[11,14,15] Based on the results of a neuropathologic study, Beach *et al.* suggested that the olfactory bulb may be a candidate region of biopsy study to

Correspondence: Shigeo Murayama, MD, PhD, Department of Neuropathology, Tokyo Metropolitan Geriatric Hospital and Institute of Gerontology, 35-2, Sakae-cho, Itabashi-ku, Tokyo 173-0015, Japan. Email: smurayam@tmig.or.jp

Received 30 March 2012; revised and accepted 19 April 2012.

confirm the diagnosis of LBD.[16] However, the biopsy of olfactory bulb is too invasive and difficult to carry out for patients without risk.[17,18]

The olfactory epithelium is composed of paraneurons and neurites from which the glomeruli of the olfactory bulb originate. However, a neuropathologic analysis of LBAS has not been carried out adequately for LBD. Duda *et al.* reported that normal α-synuclein is expressed in the basal cells, olfactory receptor neurons, supporting cells, and Bowman's glands of the olfactory epithelium in normal controls, as well as patients with Parkinson's disease, Alzheimer disease and multiple system atrophy.[19] However, pathologic α-synuclein accumulation is rare (3.7%) among both normal controls and individuals affected by DLB, Alzheimer disease or Parkinson's disease.[20] According to a biopsy study of the olfactory epithelium in individuals with Parkinson's disease and younger hyposmic controls, no specific pathologic alteration was found.[21]

Therefore, it is still controversial whether abnormal α-synuclein accumulation in the olfactory epithelium precedes the formation of LBs/LNs in the olfactory bulb and contributes to olfactory dysfunction in sporadic Parkinson's disease. The aim of this study was to clarify the neuropathologic alterations of the olfactory mucosa in LBD by immunohistochemical analysis of a series of autopsied individuals.

MATERIALS AND METHODS

Tissue source

Tissue samples were obtained from autopsy materials that were collected at the Tokyo Metropolitan Geriatric Hospital and Institute of Gerontology between October 2008 and August 2010. This hospital is located at the center of Tokyo city and is a geriatric general emergency hospital with 579 beds. This hospital provides community-based medical service to the aged population 24 h/day in cooperation with local general practitioners. The number of autopsy cases was 162 in the above duration. In addition to the general organs, we could obtain the brains and spinal cords from 105 cases in that period, that were registered to the Brain Bank for Aging Research (BBAR) with the deceased's relatives' informed consent. The BBAR is approved by the ethics committee of the Tokyo Metropolitan Geriatric Hospital and Institute of Gerontology to carry out comprehensive research.

Clinical information

All clinical information, including the presence or absence of Parkinsonism as well as dementia, was retrospectively obtained from medical charts and reviewed by two board-certified neurologists.[11,22–26] First, we evaluated Parkinsonism such as bradykinesia, resting tremor, rigidity and postural instability. In this study, when individuals had two or more of these four clinical symptoms, we defined them as having Parkinson's disease-related symptoms.[27] Second, we analyzed scores for the Mini-Mental State Examination[28] or the Hasegawa Dementia Scale (or its revised version),[29,30] the Instrumental Activities of Daily Living,[31] and the Clinical Dementia Rating (CDR).[32] When individuals were not assigned to a category of CDR, we retrospectively determined CDR using medical records, including the battery of cognitive tests above, as well as interviews with attending physicians and caregivers when necessary. Based on these results, we assigned a clinical diagnosis to each patient. The clinical diagnosis of Alzheimer disease was carried out based on the criteria of the National Institute of Neurological and Communication Disorders and Stroke-Alzheimer Disease and Related Disorders Association.[33] The diagnosis of DLB and Parkinson's disease with dementia conformed to the third report of the DLB consortium.[34]

Histology

We examined the brain and olfactory epithelium, olfactory bulb, esophagogastric mucosal junction, sympathetic ganglia, thoracic spinal cord, adrenal glands, anterior wall of the left ventricle of the heart, and abdominal skin.[22,26] The brains and spinal cords were examined as previously reported.[22,24,25] Briefly, the cerebral and cerebellar hemispheres as well as brainstem were dissected in the sagittal plane at the time of autopsy. In each case, half of the brain was preserved at −80°C for further biochemical and molecular analyses. The other half of the brain and abdominal skin were fixed in 20% buffered formalin (WAKO, Osaka, Japan) for 7–13 days and sliced in the same manner as the contralateral hemisphere. The adrenal gland and anterior wall of the left ventricle of the heart were fixed in 20% formalin. The representative areas were embedded in paraffin. Six-micrometer-thick serial sections were cut and stained with HE and KB. Sections of the amygdala, hippocampus, parahippocampal gyrus and temporal cortex were stained with the modified Gallyas-Braak method for senile plaques, NFTs and argyrophilic grains.[35]

Immunohistochemistry

Sections were immunostained using the following antibodies raised against phosphorylated tau protein (p-tau) (AT8, monoclonal; Innogenetics, Temse, Belgium): synthetic peptide corresponding to amino acids 11–28 of amyloid-beta protein (12B2, monoclonal; IBL, Maebashi, Japan); phosphorylated α-synuclein (pSyn#64, monoclonal[25] and

Table 1 Antibodies used for immunohistochemistry

Antibody	Epitope	Source	Clone	Dilution ratio	Antigen method	Retrieval (min)
pSyn#64	α-synuclein phosphorylated ser 129	T. Iwatsubo	Monoclonal	1:20000	99% formic acid	5
PSer129	α-synuclein phosphorylated ser 129	T. Iwatsubo	Polyclonal	1:100	None	
PGP9.5	PGP9.5	Biomol	Polyclonal	1:5000	microwave	30
SMI31	phosphorylated neurofilament	Sternberger	Monoclonal	1:20000	None	
Tyrosine hydroxylase	Anti-tyrosine hydroxylase, rat	CALBIOCHEM	Monoclonal	1:10	microwave	30
AT8	Phosphorylated tau protein	Innogenetics	Monoclonal	1:1000	None	
12B2	Aβ11–28	IBL	Monoclonal	1:50	99% formic acid	5

PSer129 polyclonal[36]), ubiquitin (polyclonal, Sigma-Aldrich, St. Louis, MO), Protein Gene Product 9.5 (PGP9.5, polyclonal; ENZO Life Sciences International, Farmingdale, NY USA); phosphorylated neurofilament (SMI31, monoclonal; Sternberger Immunochemicals, Bethesda, MA, USA); and tyrosine hydroxylase (Anti-Tyrosine Hydroxylase, Rat, monoclonal; Calbiochem-Novabiochem Corporation, Darmstadt, Germany) (Table 1). The signals from monoclonal and polyclonal antibodies were detected by using the automatic system on a VENTANA NX20 with the I-View DAB Universal Kit (Roche, Basel, Switzerland) according to the manufacturer's instructions. Sections were counter-stained with hematoxylin.

LBAS

CNS

In order to analyze LBAS,[22] we carried out immunohistochemical analysis with phosphorylated α-synuclein antibodies for the following sections: the medulla oblongata at the level of the dorsal motor nucleus of the vagus, the upper pons at the level of the locus coeruleus, and the midbrain including the substantia nigra, amygdala, anterior hippocampus and the peripheral nervous system from all cases (described in the next section). When immunopositive deposits were observed in these anatomic regions, we carried out additional immunohistochemical analysis for sections of the basal nucleus of Meynert, anterior cingulate gyrus, entorhinal cortex, the second frontal and temporal gyri and the supramarginal gyrus, using antibodies raised against phosphorylated α-synuclein.

Peripheral nervous system

To analyze LBAS of the peripheral nerve, tissue sections from epicardium and epicardial fat of the left ventricle of the heart, sympathetic ganglia, esophagogastric mucosal junction, adrenal gland[22] and abdominal skin[26] were examined by using antibodies raised against phosphorylated α-synuclein.

Olfactory mucosa

At the time of autopsy, the olfactory mucosa, bony septae and contiguous cribriform plate were removed en bloc (Fig. 1). The cribriform plate was dissected in the sagittal plane of the midline by using an electric jigsaw. The left side was fixed for 24 h in 4% paraformaldehyde. After fixation, the olfactory mucosa was removed, dehydrated in a graded alcohol series, cleared in xylene and embedded in paraffin. The right side was fixed for 24 h in 4% paraformaldehyde, decalcified with EDTA for 2 weeks, and dehydrated and embedded in paraffin. Serial 6-μm-thick sections were stained with HE and immunolabeled with antibodies against phosphorylated α-synuclein, PGP9.5, phosphorylated neurofilament, tyrosine hydroxylase, phosphorylated tau and amyloid β (Table 1). In particular, the olfactory receptor neurons of the olfactory epithelium were identified by using PGP9.5 immunohistochemistry.[19] The normal anatomical appearance of the olfactory system is shown in Figure 2.

Olfactory bulb

The olfactory bulbs were prepared for histologic sections to analyze the presence of LBAS. By using HE stain and α-synuclein antibodies, LBAS were identified in the glomeruli, mitral cells, tufted cells and granular cells as previously reported.[11] Mitral and tufted cells were distinguished by their specific shapes. Each neuron was identified when it had an apparent nucleus containing a prominent nucleolus and Nissl substance.

Semiquantitative scoring system of Lewy-related pathology

For each section, we semi-quantitatively graded the immunohistochemical staining with antibody raised against phosphorylated α-synuclein. Our grading system was modified based on the scoring system of the third report of the DLB consortium[34] because we used both the HE stain and immunohistochemistry using monoclonal antibody for phosphorylated α-synuclein to identify LBAS.

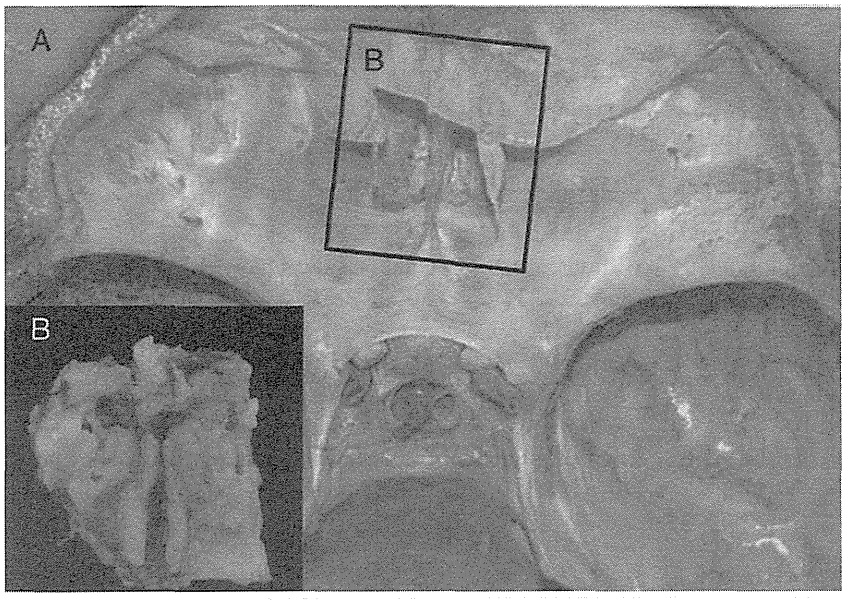

Fig. 1 (a) The anterior cranial fossa after removal of the brain. In order to obtain the olfactory mucosa, the bony septae and contiguous cribriform plate (the rectangular area) were dissected using an electric jigsaw. (b) An inset shows the olfactory mucosa and cribriform plate from the opposite side of the rectangular area.

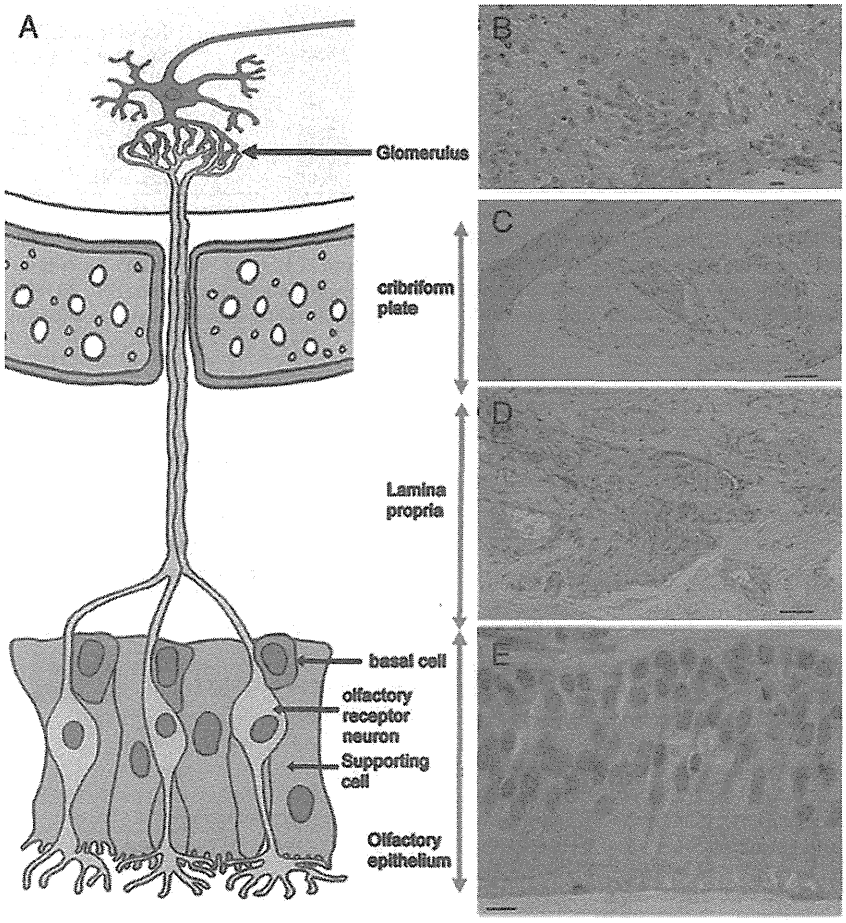

Fig. 2 Scheme of the normal olfactory pathway (a) and photomicrographs of representative histologies of each region (b–e). The olfactory epithelium is composed of three cell types: the basal cells, olfactory receptor neurons and supporting cells (a). The basal cells are the progenitor of the olfactory receptor neurons (a, e). In general, the turnover rate of the olfactory receptor neurons is approximately 30–90 days. Nerve fibers are present in the lamina propria and cribriform plate (c and d, respectively). They consist of either the axons of the olfactory receptor neurons or postganglionic sympathetic nerve fibers. There are glomeruli in the olfactory bulb (b). Glomeruli are the synaptically connected structures of the axons of the olfactory receptor neurons and mitral/tufted cells in the olfactory bulb. (b, e), scale bar = 10 μm; (c), scale bar = 50 μm; (d), scale bar = 100 μm.